Ehtezazi, T, Algellay, M, Islam, Y, Roberts, M, Dempster, NM and Sarker, SD

The Application of 3D Printing in the Formulation of Multilayered Fast Dissolving Oral Films.

The Application of 3D Printing in the Formulation of Multilayered Fast Dissolving Oral Films

Touraj Ehtezazi*, Marwan Algellay, Yamir Islam, Matt Roberts, Nicola M Dempster, Satyajit D Sarker,

School of Pharmacy and Biomolecular Sciences, Liverpool John Moores University, Byrom Street, Liverpool, L3 3AF, UK.

* Corresponding Author

e-mail t.ehtezazi@ljmu.ac.uk

Abstract

Fast dissolving oral films (FDFs) provide an alternative approach to increase consumer acceptance by advantage of rapid dissolution and administration without water. Usually FDFs require taste-masking agents. However, inclusion of these excipients could make developing the formulation a challenging task. Hence, this work employed fused-deposition modelling three-dimensional (FDM 3D) printing to produce single-layered (SLFDFs), or multilayered (MLFDFs) films, with taste-masking layers being separated from drug layer. Filaments were prepared containing polyethylene oxide (PEO) with ibuprofen or paracetamol as model drugs at 60°C. Also filaments were produced containing polyvinyl alcohol (PVA) and paracetamol at 130°C. Furthermore, a filament was prepared containing PEO and strawberry powder for taste-masking layer. FDFs were printed at temperatures of 165°C (PEO) or 190ºC (PVA) with plain or mesh designs. HPLC and mass-spectroscopy analysis indicated active ingredient stability during film preparation process. SLFDFs had thicknesses as small as 197±21µm, and MLFDFs had thicknesses starting from 298±15µm. Depending on the formulation and design, mesh SLFDFs presented disintegration time as short as 42±7s, and this was 48±5s for mesh MLFDFs. SLFDFs showed drug content uniformity in the range of 106.0%-112.4%. In conclusion, this study provides proof-of-concept for the manufacturing of FDFs by using 3D printing.

1. Introduction

Fast dissolving oral films (FDFs) provide the opportunity to administer medicines and avoid first-pass metabolism.[1] FDFs may also be used in children[2,3], patients with dysphagia[4] and elderly patients.[5] Although certain products such as paracetamol are available as oral suspension, these contain additives and sugar which may not be advisable for children.[6] In addition, administrating oral liquid formulations to children is challenging by using syringes.[7] These concerns are triggers for development of more number of FDF formulations.

FDFs are manufactured by hot melt extrusion or solvent casting methods, with the latter process being popular.[8,9] The application of hot-melt extrusion process is growing due to its solvent-free, continuous production, and less chance of drug instability as the result of not using solvents.[8] In the formulation of FDFs rapid dissolution/release of the drug is required, and at the same time masking the drug taste is extremely important. Although there are handful of sweeteners and taste-masking agents, the presence of another ingredient in the mixture of formulation may significantly affect the physicochemical properties of the resulting paste/film. Consequently, further formulation adjustments/improvements are needed.[9] Moreover, there are challenges in the development and manufacture of FDFs. These include: achieving desired FDF weight uniformity, chemical stability of active ingredient/excipients during manufacturing process, increasing film thickness due to the die swell phenomena, and the non-homogenous flow of powder/paste in the extrusion chamber.[8,10,11]

Three-dimensional (3D) printing has been employed in the development of complex oral dosage forms,[12-19] and at commercial scale for the production of Spritam® fast dissolving tablet.[20,21] Hence, 3D printing may become an option to develop and manufacture desired FDFs by overcoming limitations of current FDF manufacturing techniques. In particular, 3D printing fused-deposition modelling (3D FDM) is closer to the hot-melt extrusion process. 3D FDM has been employed to develop various oral drug delivery systems.[17,22-28]

Conventional FDM 3D printers utilise filaments to produce the desired objects. In this equipment, the filament passes through a narrow tubing system and rotating pulleys/gears in the 3D printer head. Here, the filament is heated and extruded through a nozzle with narrow diameter (typically 0.4 mm). FDM 3D printers can produce objects with reproducible dimensions, in particular when filaments are used with uniform diameters (low diameter tolerance).[17] If there is an inconsistency in diameter of the filament (being too wide or too thin), either the printed object would have irregular dimensions and weight, or the extruder would fail to print. Hence, 3D FDM could potentially allow manufacturing FDFs with reproducible dimensions and physicochemical properties. In addition, 3D FDM provides the opportunity of laminating more than one-layer in a film. Then, these hypotheses have been examined in this paper. In the present work, 3D FDM was employed to produce 3D FDFs with taste-masking layers being printed on the drug-containing layer, and also to create mesh design of FDFs to reduce disintegration time. This property of 3D FDFS was compared to a commercially available FDF.

2. Materials and Methods

2.1. Materials

Paracetamol, polyvinyl alcohol (PVA, Mw 89,000-98,000, 99+% hydrolysed), polyethylene oxide (PEO) Mw 100,000 Da, PEO Mw 200,000 Da, poly (ethylene) glycol (PEG) Mw 4000 Da, and PEG Mw 30,000 Da were purchased from Sigma Aldrich UK. Ibuprofen was supplied by BASF SE (Ludwigshafen, Germany). Starch was obtained from BDH Chemicals (Poole, England). Sodium starch glycolate was purchased from Shin-Etsu (Tokyo, Japan). Croscarmellose sodium was acquired from FMC Europe N.V. (Brussels, Belgium). Sodium lauryl sulphate (SLS) was supplied by Janssen Pharmaceuticals (Beerse, Belgium). Freeze dried strawberry powder was purchased from Healthy Suppliers (Hove, UK). Solvents were analytical grade.

2.2. Preparation of Filaments

The compositions of formulations are illustrated in Table 1. Drug and excipients were ground using pestle and mortar to form fine powder and then mixed together for 15 minutes utilising a turbula mixer (Type 2B, WAB, Muttenz, Switzerland). The contents were transferred to a single-screw Noztek Pro Filament Extruder (Noztek, Shoreham, UK) with the temperatures set at 60°C for PEO and 130°C for PVA. The nozzle die diameter was 1.6 mm. The extruder was placed at a height, which provided constant gravity pull on the extrudate to achieve straight filaments with uniform diameter. As the filament was extruded, the diameter was measured every 5-10 cm utilising a digital vernier caliper (RS Pro, Corby, UK) to ensure uniformity of the filament. The optimum diameter was between 1.60 – 1.80 mm. If the digital vernier caliper measurements indicated that the filament diameter became greater than this range, then an object with the weight of one gram was added to the first part of the extruded filament to increase the gravitational force on the extrudate. This was to maintain the desired diameter of the filament. The optimum diameter of the filament was crucial for using in the 3D printer (section 2.3). Preliminary studies showed that PEG with molecular weight of 30 kDa produced brittle filaments and only PEO 100 kDa and 200 kDa produced suitable filaments. Based on these observations, PVA with large molecular weight was considered. In addition, it was found that SLS improved drug release rate from films containing PEO. Starch and super disintegrating agents (i.e., sodium starch glycolate and croscarmellose) were added to the formulations to aid disintegration of films.

2.3. 3D Printing of FDFs

The films were printed using a fused-deposition modelling (FDM) Wanhao Duplicator 4 Desktop 3D printer (Jinhua, Zhejiang, China), and SolidWorks 3DCAD (Dassault Systèmes SolidWorks Corp, Waltham, Massachusetts, USA) was used to design the film. The printer head included extruder nozzle with diameter of 0.4 mm. The shapes of films are provided in Table 1. The circular films were designed with the diameter of 20 mm and thickness of 0.2 mm. The square films were designed with the length of 20 mm (the same width), and the height of 0.2 mm. Mesh films were printed as square shape, to reduce the complexity of designing films. MakerWare software (version 2.2.2.89, Brooklyn, NY, USA) was utilised to export the design into the printer. Printer extrusion parameters were: 40% infill for PEO films and 100% infill for PVA films, two shells, 0.10 mm layer height, extruder temperature 165ºC for PEO films and 190°C for PVA films, extruder speed 70 mm/s for PEO films and 90 mm/s for PVA films, and with travelling speed of 60 mm/s for PEO films and 150 mm/s for PVA films. The

infill of 40% or 100% was chosen to achieve high density films with suitable mechanical strengths and adherence to the surface of 3D printer bed. Although hexagonal infill was the infill pattern, preliminary studies indicated that the infill pattern started to appear after printing first few layers on the printer bed. Sticky masking blue tape (3M™) was utilised to facilitate the adhesion of printed films on the printer bed. The printer bed temperature was not altered (kept at room temperature). Printing time was two minutes for single-layer plain film, while the printing time was 30s for mesh film. The taste masking layer was designed in the MakerWare software at the same position of the drug containing layer but with 0.2 mm above the platform. Therefore, after printing the drug containing layer utilising one of the printer heads, the taste masking layer was printed on the drug containing layer using the other printer head.

2.4. Differential Scanning Calorimetry (DSC) and Fourier Transform Spectroscopy (FTIR)

DSC analysis (Perkin Elmer DSC 7 Waltham, Massachusetts, USA) was carried out on starting powders, filaments and films. Samples were accurately weighed and subsequently were enclosed in aluminium crimped crucibles. Initially samples were cooled to 0 °C at the rate of 20°C/min, and held for 1 minute and then samples were heated from 0 to 90°C at 20°C/min for samples containing ibuprofen, from 0°C to 140°C at 20°C/min for samples containing paracetamol or PVA. In addition, the samples were cooled down again to 0°C and heated to 220°C at the rate of 20°C/min for samples containing paracetamol or PVA. This was to simulate the heating procedure during 3D printing. FTIR was conducted on samples using a Perkin Elmer Spectrum BX II (Norwalk, CT, USA).

2.5. Mass Spectroscopy (MS)

Waters Micromass LCT mass spectrophotometer (Milford, Massachusetts, USA) was employed, which was also attached to Harvard apparatus pump 11. Nebulizer gas flow was used at 26 L/hr, desolvation gas flow at 789 L/hr, with desolvation temperature of 200ºC, capillary voltage at 3200 V, and extraction cone voltage at 3 V. Electrospray ionization was achieved by applying voltage of 35V. Desolvation was achieved by using nitrogen gas purging at 700 L/hr. Sample infusion flow rate was 20 µL/min. Samples for each formulation containing ibuprofen were prepared by dissolving 5 mg of powder, filament, or film with 5 ml of purified methanol, sonicated for 10 minutes; and the solution was filtered using 0.2µm Sartorius filters. Samples of powder, filament or film containing paracetamol with PVA were dissolved in water: methanol (50:50) solution.

2.6. High Performance Liquid Chromatography (HPLC)

An Agilent 1200 series HPLC (Stockport, Cheshire, UK) was used to analyse the drug content of the powders, filaments and films. To quantify ibuprofen, a C18 column was used with a mobile phase consisting of: 0.5 volumes of phosphoric acid, 340 volumes of acetonitrile and 600 volumes of water then equilibrate and dilute to 1000 volumes with water. Weighed amount of ibuprofen standard and ibuprofen containing samples were dissolved in 2 mL of acetonitrile separately, and sonicated for 10 minutes. The resulting solution was diluted to 10 mL by using the mobile phase. The flow rate was set at 2 mL/min, and the detection spectrophotometer was set at 214 nm with injection volume of 20 µL.

Weighed amounts of the paracetamol standard and samples were transferred into volumetric flask containing mobile phase (3:1, methanol: water), sonicated for 2 minutes. Flow rate was set at 1.5 mL/min; detection spectrophotometer was set at 243 nm, and sample volume was 10 µL. The stationary phase comprised of a C-18 column, µbondapak (300 mm×3.9 mm; Waters®, USA). The content uniformity was conducted only for formulation E (PVA films containing paracetamol). A calibration curve was prepared for paracetamol with a linear relationship between 0.017-1.56 mg/mL (R^2 = 0.9976). Three films were analysed.

2.7. Film Thickness

The thickness of each film was determined by using a digital vernier caliper supplied by RS Pro (Corby, UK). Thickness of each film was measured from four directions.

2.8. Tensile Properties

Tensile testing was conducted using a TA-XT-Plus® texture analyser (Stable Microsystems Texture Analyser, London, UK). For the purpose of this test, longer films were printed. All the films tested had a uniform size of 100 mm×20 mm. This was to ensure that the instrument would be able to break the film (wider films were too strong for the machine). Each test strip was longitudinally placed in the tensile grips on the texture analyser, and the sequence of "Return to Start" was elicited. Initial grip separation was 40 mm and separation speed was set at 20 mm/s. The tensile strength was calculated from the following equation (1):

$$Tensile\ Strength\ (Pa) = \frac{Force\ at\ Break\ (N)}{Cross\ Sectional\ Area of\ Sample\ (m^2)} \quad (1)$$

Values are expressed as mean ± standard deviation (n=3).

2.9. Scanning Electron Microscopy

3D printed films were sputter coated with gold using an Emitech K550 (Ashford, UK) coater and then visualized with a Philips XL20 (Eindhoven, Holland) scanning electron microscope (SEM).

2.10. In vitro Dissolution Studies

Dissolution studies (paddle method) were carried out on three (containing PVA) or six (containing PEO) films of each formulation using the United States Pharmacopeia dissolution apparatus II (Varian VK 7000, Agilent Technologies, CA, USA) at 50 rpm, in 900 mL of phosphate buffer (pH 7.4 for ibuprofen and pH 5.8 for paracetamol). The release media were maintained at 37.3 ± 0.5°C. The amounts of active ingredients were measured using Cary 50 UV-Vis spectrophotometer (Agilent Technologies, CA, USA) with wavelength of 243 nm for paracetamol and 265 nm for ibuprofen. For standard solutions, 100 mg of active ingredient was dissolved in 1000 mL volume of the buffer. The percentage of released drug and time for maximum drug release were recorded for each formulation. Results are presented as mean ± standard deviation.

2.11. Disintegration Tests

Disintegration time of each 3D film was determined in distilled water at 37 ± 0.5ºC using Copley Scientific disintegration tester DTG 1000 (Copley Scientific, Nottingham, United Kingdom). Each film was placed in the tube over the 2 mm size mesh with disintegration disk

on it. The time was recorded for each film to disintegrate and pass the residue completely through the wire mesh. Three films were tested from each formulation.

2.12. Powder X-ray Diffraction (PXRD) Analysis

PXRD analysis was carried out on PVA pure powder, paracetamol pure powder, formulation G powder mixture, filaments and films of formulation G with the help of MiniFlex XRD (Riagaku, Japan). The PXRD analysis was carried out using the Cu K-alpha radiation ($\lambda = 1.54$ Å) at 15 mA and 30 kV. The samples were scanned between the 2θ angle ranging from 5.0° to 55° at the 0.01° step size (2θ) and scan step time of 2 seconds. RIGAKU data viewer software was used for data analysis.

3. Results

3.1. The morphology of FDFs

Figure 1 presents photographic images of typical FDFs that were manufactured by 3D printing, and also corresponding SEM images. These show that films had two different surface morphologies. One side of the film had smooth surface, which was in contact with the printer bed. The other side had a porous structure. The presence of porous structure within the films may contribute to the rapid disintegration of the dosage form. Multilayered FDFs presented acceptable integrity of the taste-masking layers over drug containing layer (core layer). Also, it was needed to manufacture the strawberry filament with PEO at 70ºC to prevent charring of the flavouring agent. The films presented acceptable flexibility, and mesh FDFs were the most flexible samples with the ability to bend 90º with no obvious cracks on the films. This was considered as a typical deformation of the film, which may occur during packaging or handling. However, further deformations cracked the films.

3.2. Weight and Thickness Uniformity of FDFs

Table 2 presents the weight uniformity of FDFs, and thickness uniformity within a single film. It can be seen that the thickness variation was less than 4% within films, and weight uniformity was greater than 97%, apart from the formulation F, which was multilayered plain film. In this table, the results of Listerine®POCKETPAKS® breath strips are also presented. It can be seen that amongst 3D FDFs only mesh films had short disintegration time (42s ± 7s for single-layered film and 48s ± 5s for double-layered film). However, these were higher than the disintegration time of the Listerine®POCKETPAKS® breath strips (14s ± 2s). PEO films became brittle during storage under ambient conditions. On the other hand, PVA films maintained their mechanical strengths under similar storage conditions. Furthermore, data in Table 2 indicates that polymers with lower molecular weight such as PEO 100k Da would achieve faster disintegration time compared to the same formulation but including polymers with larger molecular weight (such as PEO 200k Da). Table 2 also presents the dose contents of the films, and it can be seen that mesh films contained less drug compared to plain films, due to their particular designs.

3.3. DSC Analysis of FDFs

Figure 2A presents DSC thermograms of pure ibuprofen, PEO 100k Da, and PEO 200k Da powders. It can be seen that ibuprofen melted at 79.3°C, and PEO 100k and PEO 200k melted

at 71.6°C and 72.6°C, respectively. Figure 2B illustrates the DSC thermograms of Formulation B for powder mixture, as filament and as film. It can be seen that the film or filament melted at lower temperatures (54.1°C and 55.2°C, respectively) compared to original powder forms. These suggest the dispersion of drug at molecular levels within the films or filaments. The formulation powder mixture melted at approximately 69°C, which was lower than melting temperature of ibuprofen, PEO 100 kDa and PEO 200k Da. DSC data also suggested dispersion of paracetamol at the molecular levels within PVA filament or film. The melting peak of paracetamol was observed only in the DSC thermogram of powder mixture, not in filament or film (provided in supplementary information, Figure S3). The DSC thermograms are presented for paracetamol and PVA in supplementary information (Figures S1 and S2).

3.4. Powder X-Ray Diffraction (PXRD) analysis

The diffractogram of pure paracetamol powder presented a series of intense peaks, indicating of its crystalline nature (Figure 3A). On the other hand, the PXRD analysis of PVA showed only diffraction peaks at 20° and 40°, suggesting some crystallinity (Figure 3A). The diffractogram of PVP-paracetamol mixture powder (formulation G) showed diffraction features for both of powders superimposed on the broad background (Figure 3B). However, the filament and the film patterns were characterised by diffraction peaks at 20° and 40°, indicating presence of crystalline PVA aggregates (Figure 3B). This analysis further supported dispersion of paracetamol at molecular level within the filament and film.

3.5. FTIR Analysis of FDFs

FTIR results showed stability of the formulation ingredients during manufacturing of the films. Figure 4 presents typical examples of FTIR spectra for paracetamol with PVA (formulation G), as powder mixture, filament and film. Analysing the peaks shows presence of hydroxyl groups of PVA at wavenumbers of 3321 cm^{-1}, in powder formulation and slight modifications (3294 cm^{-1}) in the filament and film preparations. This could be due to the interactions of O-H groups of PVA with O-H group of paracetamol. This data also indicated the stability of paracetamol during manufacturing process of 3D FDFs. Similar trends were also observed for formulations containing ibuprofen (supplementary information, Figure S4). The FTIR spectra of pure paracetamol, PVA, PEO 100, PEO 200, and ibuprofen powders are provided in supplementary information (Figures S5-S9).

3.6. Mass Spectroscopy and HPLC Analysis of FDFs

In order to evaluate the stability of active ingredient in the manufacturing process, the mass-spectra were obtained for formulation powder mixture, filament and film. Figure 5 presents mass-spectra of formulation C as powder mixture, filament and FDF. It can be seen that ibuprofen had a peak at m/z=229.0693 (ibuprofen + Na), and this can also be found in the spectra of filament and film. These outcomes indicated that the active ingredient remained chemically stable in the manufacturing process by the 3D printing method. Mass spectra of paracetamol in the filament and film also showed the stability of the active ingredient during preparation process of 3D FDF (supplementary information Figure S10). In addition, HPLC analysis confirmed the stability of ibuprofen and paracetamol in the manufacturing processes of filaments and films containing PEO (provided in supplementary information, Figures S11-

S15). Furthermore, we carried out the HPLC analysis of the 3D FDFs containing PVA for determining the amounts of paracetamol, and to detect any drug degradation. It was observed that the films showed the paracetamol peak at the same retention time as the standard drug molecule (Figures S16 and S17). Thereby confirming that the paracetamol did not degrade in the printing process. In addition, drug contents in the films were evaluated for formulation E; and the values were found to be between 106.0% and 112.4% (109.6% ± 3.2%, mean ± standard deviation) of nominal drug content (15.6 mg per film).

3.7. In vitro Dissolution Tests

Figure 6 illustrates the in vitro release profiles of plain and mesh 3D FDFs (formulations C, E, F, G and H). The data shows that formulations C, G and H had faster drug release compared to formulations E and F. This data shows that drug release rate may be increased by optimising the design of the films (by manufacturing them as mesh). Also, it can be seen from Figure 6 that adding taste-masking layers for plain films (formulation F) delayed the drug release significantly compared to core plain films (formulation E). However, this can be avoided by manufacturing films in a perforated shape (such as mesh). Films of formulations A, B, and D had similar drug release profiles (supplementary information, Figure S18).

3.8. Tensile Strength

The 3D films showed suitable mechanical strengths immediately after manufacturing. However, as mentioned previously, PEO films became brittle up on storage under ambient conditions. On the other hand, PVA 3D films maintained suitable mechanical strengths on storage under similar conditions. The tensile strength was 2.5 ± 0.03 MPa for 3D films of formulation E. While the tensile strengths were 0.57 ± 0.05 MPa and 1.27 ± 0.10 MPa, for single-layered mesh film (formulation G) and double-layered mesh film (formulation H), respectively. Figure 7 presents the texture profile analysis plots of the formulations G and H, and the saw-tooth curves were typical characteristics of mesh 3D films. Accordingly, plain 3D FDFs showed a single peak in the texture profile analysis plot (supplementary information, Figure S19). As expected, Figure 7 presents that films of formulation H (with taste-masking layer) were stronger than formulation G films (single-layered).

4. Discussion

This study showed proof-of-concept in preparing FDFs by 3D-printing. Depending on the design, 3D-films disintegrated on average between 42.2s and 150.0s. This range covers films manufactured by the hot melt extrusion method.[11] However, 3D FDFs presented disintegration time longer than the disintegration time for a commercially available FDF (Listerine®POCKETPAKS® breath strips), or FDFs prepared by the solvent-casting method.[11] On the other hand, 3D FDFs showed both rapid and extended drug release profiles as seen previously for films prepared by solvent-casting or hot-extrusion methods.[11,29] As expected, 3D printing allowed layers of different compositions to be added on films. It should be noted that manufacture of layered oral films have been achieved previously by employing solvent casting method.[30-32] However, the films manufactured by the 3D method (in particular mesh designs) had more thickness uniformity than layered films prepared by the solvent casting method. [32]

In this study, we found that paracetamol was stable at extrusion temperature of 130°C (for formulations containing PVA) and printing temperature of 190°C (films containing PVA). Also, previous works have shown the stability of active ingredients during FDM 3D printing.[25,26] However, in this work, the taste-masking agent charred at temperature of 130°C. Therefore, separate filaments were prepared at a lower temperature that contained the taste-masking agent; and this was printed on the drug containing layer to form multilayered FDFs. Nevertheless, the stability of the taste-masking agent should also be evaluated during the entire manufacturing process. Furthermore, additional studies will be required by employing volunteers or Electronic Tongue[9] to evaluate the performance of the taste-masking layers.

The drug release profiles of 3D FDFs depended on the design and presence of taste-masking layer. Plain FDFs with taste-masking layers showed significantly slower drug release rate compared to plain FDFS without the taste-masking layers. This could be due to the taste-masking layer that acted as a barrier for drug molecules reaching the release media. 3D FDFs showed faster drug release compared to previously reported FDFs prepared by the hot extrusion method.[11] This could be due to the presence of microcrystalline cellulose in the formulation to prevent the adherence of the paste to the extruder.[11] On the other hand, plain 3D FDFs presented slower drug release compared to FDFs prepared by the solvent casting method. [4,11,29] This could be due to utilising polymers with large molecular weights for the 3D printing. However, this drawback was alleviated by printing the films in a mesh format. It should be added that printing FDFs in the mesh format resulted in the reduction of the drug content. Therefore, this may limit administrating large doses as mesh design of 3D FDFs. Furthermore, hot melt extrusion has been employed to develop PEO based buccal films.[33] However, drug release was faster from 3D films containing PEO compared to the buccal films. The difference could be due to the different film thicknesses. The buccal films had 0.5 mm thicknesses,[33] while 3D FDFs had smaller thicknesses.

In this work the PEO based 3D films were printed at 40% infill, and PVA based 3D films at 100% infill. However, PEO printed films appeared compact. As it is explained in section 2.3 (3D Printing of FDFs), from preliminary studies we learned that first printed layers did not take into account either the infill percentage or infill pattern. Perhaps this was due to the formation of a wall of the printed object. Since printed films in this work were thin, therefore, two parameters (infill percentage and infill pattern) did not affect on the structure of the films. However, infill pattern and infill percentage are important parameters that could be investigated further to evaluate the effects of these parameters on the mechanical strengths and disintegration time of the films.

It was observed that PEO 3D films became fragile during storage under ambient conditions, while 3D PVA films maintained their mechanical strength despite of PVA being a hydrophilic polymer. Oxidation of PEG by air in a wet environment has been shown before.[34] In addition, a previous work investigated the effects of different storage conditions on the mechanical properties of PEO buccal films.[33] This study found that the mechanical properties of PEO films changed significantly under 75% relative humidity (RH) storage conditions.[33] As the RH was usually more than 75% in the ambient condition of where 3D FDFs were stored, then the results

of the previous study[33] support fragmentation of PEO based 3D FDFs during storage under ambient conditions.

PVA and PEO have been utilised successfully in the manufacture of drug delivery systems utilising 3D FDM. [17,26,28] In particular, PVA and PEO have been employed to manufacture disks by applying 3D FDM with infill of 100%.[28] Furthermore, hydroxypropyl cellulose (HPC) and hydroxypropyl methyl cellulose (HPMC) have been employed to manufacture buccal films by applying the hot melt extrusion method,[35,36] and disks by applying 3D FDM.[28] Then, 3D printing may be employed to investigate these polymers for the manufacture of buccal films or fast dissolving oral films.

Plasticisers are incorporated into the formulations of FDFs to achieve a suitable flexibility.[11,29,37,38] PEG 400, glycerol and propylene glycol[39] are amongst used plasticisers. PEG 400[23] and glycerol[28] also have been utilised in the manufacture of drug delivery systems utilising 3D FDM. However, in the manufacture of FDFs by FDM 3D printing, a certain mechanical strength (stiffness) of the filament was necessary in order to be used in the 3D printer. Therefore, in this study, plasticisers were not used, but 3D FDFs showed an acceptable flexibility suitable as an oral film.

DSC thermograms of 3D FDFs suggested miscibility of the active ingredients with excipients in the formulation, which also have been observed in previous studies in preparing FDFs by solvent casting method.[4,40] As a result, 3D FDFs met the weight uniformity that is required by pharmacopeia.[41] This is apart from formulation F, which was 3-layered FDF. In addition, 3D FDFs showed the uniformity of content in the range of 106.0% to 112.4%, which was also in the range required by pharmacopeia (85%-115%).[41] It should be noted that pharmacopeia requires ten samples to be tested. Therefore, 3D FDM could produce FDFs that meet the weight uniformity and the uniformity of contents required by pharmacopeia.

5. Conclusions

This paper shows proof-of-concept for 3D printing of fast dissolving oral films. 3D FDFs achieved weight uniformity and the uniformity of contents required by pharmacopeia. Also 3D printing allowed producing mesh design of FDFS to reduce the disintegration periods. Although the 3D FDFs were printed at high temperatures (165°C or 190°C), the drug molecules were stable. However the taste-masking agent was unstable. Therefore, it was deposited as a separate layer at a lower temperature on the drug-containing layer. Although FDFs can be produced either by hot-extrusion or solvent casting methods, 3D printing could reduce the development or production time.

The manufacturing of strong filaments required utilising large molecular weight polymers, which delayed the disintegration time of plain 3D FDFs. Therefore, optimised FDM 3D printers that do not require utilising filaments may overcome this problem.

Acknowledgment

We would like to thank Noztek for technical support in optimising the extrusion process and equipment maintenance. Also we are grateful for technical assistance of Miss Debaprita Das.

Conflict of Interest

The authors stated they had no conflict of interest.

List of Figures

Figure 1. Photographic images of films made from formulation H, formulation G, and formulation C (top row). Underneath of each photographic image, corresponding SEM photomicrograph is also presented. (SLFDF: single-layered fast dissolving oral film; MLFDF: multilayered fast dissolving oral film).

Figure 2. A) DSC thermograms of ibuprofen, PEO 100k, and PEO 200k as pure powders. B) DSC thermograms of formulation B (containing PEO 200k) as powder mixture, filament and film. It can be seen that the DSC thermogram of ibuprofen disappears in the formulations as film or filament, indicating dispersion of ibuprofen molecules within PEO polymer.

Figure 3. The powder X-ray diffraction patterns. A) Pure paracetamol powder (1) and pure PVA powder (2). B) Powder mixture of paracetamol and PVA (formulation G) (1), filament (2), and film (3).

Figure 4. FTIR spectra of formulation G, as powder mixture, filament and film. These spectra suggest interactions between OH groups of PVA and paracetamol as filament or film, and the stability of the active ingredient during manufacturing of 3D FDFs.

Figure 5. Mass-spectra of formulation C as film (top), filament (middle), and as powder mixture (bottom). These spectra illustrate the stability of ibuprofen during manufacturing process of FDF by 3D printing.

Figure 6. The in vitro drug release profiles of 3D printed films (formulations C, E, F, G, H). Bars indicate standard deviations.

Figure 7. Texture profile analysis plots of formulations G and H films, presenting higher tensile strength of formulation H film (mesh double-layered) compared to formulation G film (mesh single-layered). The saw-tooth profiles were due to the mesh designs of films.

References

1. Abdelbary A, Bendas ER, Ramadan AA, Mostafa DA. Pharmaceutical and pharmacokinetic evaluation of a novel fast dissolving film formulation of flupentixol dihydrochloride. AAPS PharmSciTech. 2014; 15(6):1603-1610.
2. Zhang HH, Mei-Gui; Wang, Yun; Zhang, Jie; Han, Zi-Ming; Li, Shu-Jun. Development of Oral Fast-Disintegrating Levothyroxine Films for Management of Hypothyroidism in Pediatrics. Trop J Pharm Res. 2015; 14(10):1755-1762.
3. Slavkova M, Breitkreutz J. Orodispersible drug formulations for children and elderly. Eur J Phar Sci. 2015; 75:2-9.
4. Satyanarayana DA, Keshavarao KP. Fast disintegrating films containing anastrozole as a dosage form for dysphagia patients. Arch Phar Res. 2012; 35(12):2171-2182.
5. Londhe VY, Umalkar KB. Formulation development and evaluation of fast dissolving film of telmisartan. Indian J Pharm Sci. 2012; 74(2):122-126.

6. Feketea G, Tsabouri S. Common food colorants and allergic reactions in children: Myth or reality? Food chemistry. 2014; 230:578-588.
7. van Riet-Nales DA, Ferreira JA, Schobben AFAM, de Neef BJ, Egberts TCG, Rademaker CMA. Methods of administering oral formulations and child acceptability. Int J Pharm. 2015; 491(1):261-267.
8. Jani R, Patel D. Hot melt extrusion: An industrially feasible approach for casting orodispersible film. Asian J Phar Sci. 2015; 10(4):292-305.
9. Cilurzo F, Cupone IE, Minghetti P, Buratti S, Selmin F, Gennari CGM, Montanari L. Nicotine Fast Dissolving Films Made of Maltodextrins: A Feasibility Study. AAPS Pharm Sci Tech. 2010; 11(4):1511-1517.
10. Bala R, Pawar P, Khanna S, Arora S. Orally dissolving strips: A new approach to oral drug delivery system. Int J Pharm Investig. 2013; 3(2):67-76.
11. Cilurzo F, Cupone IE, Minghetti P, Selmin F, Montanari L. Fast dissolving films made of maltodextrins. Eur J Pharm Biopharm. 2008; 70(3):895-900.
12. Goyanes A, Chang H, Sedough D, Hatton GB, Wang J, Buanz A, Gaisford S, Basit AW. Fabrication of controlled-release budesonide tablets via desktop (FDM) 3D printing. Int J Pharm. 2015; 496(2):414-420.
13. Skowyra J, Pietrzak K, Alhnan MA. Fabrication of extended-release patient-tailored prednisolone tablets via fused deposition modelling (FDM) 3D printing. Eur J Pharm Sci. 2015; 68:11-17.
14. Goyanes A, Buanz AB, Basit AW, Gaisford S. Fused-filament 3D printing (3DP) for fabrication of tablets. Int J Pharm. 2014; 476(1-2):88-92.
15. Khaled SA, Burley JC, Alexander MR, Roberts CJ. Desktop 3D printing of controlled release pharmaceutical bilayer tablets. Int J Pharm. 2014; 461(1–2):105-111.
16. Khaled SA, Burley JC, Alexander MR, Yang J, Roberts CJ. 3D printing of five-in-one dose combination polypill with defined immediate and sustained release profiles. J Control Release. 2015; 217:308-314.
17. Goyanes A, Buanz AB, Hatton GB, Gaisford S, Basit AW. 3D printing of modified-release aminosalicylate (4-ASA and 5-ASA) tablets. Eur J Pharm Biopharm. 2015; 89:157-162.
18. Khaled SA, Burley JC, Alexander MR, Yang J, Roberts CJ. 3D printing of tablets containing multiple drugs with defined release profiles. Int J Pharm. 2015; 494(2):643-650.
19. Sandler N, Salmela I, Fallarero A, Rosling A, Khajeheian M, Kolakovic R, Genina N, Nyman J, Vuorela P. Towards fabrication of 3D printed medical devices to prevent biofilm formation. Int J Pharm. 2014; 459(1-2):62-64.
20. Norman J, Madurawe RD, Moore CM, Khan MA, Khairuzzaman A. A new chapter in pharmaceutical manufacturing: 3D-printed drug products. Adv Drug Deliv Rev. 2017; 108:39-50
21. United States Food and Drug Administration, Highlights of Prescribing Information Spritam, 2015 Available from http://wwwaccessdatafdagov/drugsatfda_docs/label/2015/207958s000lblpdf.
22. Okwuosa TC, Stefaniak D, Arafat B, Isreb A, Wan KW, Alhnan MA. A Lower Temperature FDM 3D Printing for the Manufacture of Patient-Specific Immediate Release Tablets. Pharm Res. 2016; 33(11):2704-2712.
23. Okwuosa TC, Pereira BC, Arafat B, Cieszynska M, Isreb A, Alhnan MA. Fabricating a Shell-Core Delayed Release Tablet Using Dual FDM 3D Printing for Patient-Centred Therapy. Pharm Res. 2017; 34(2):427-437.
24. Goyanes A, Wang J, Buanz A, Martinez-Pacheco R, Telford R, Gaisford S, Basit AW. 3D Printing of Medicines: Engineering Novel Oral Devices with Unique Design and Drug Release Characteristics. Mol Pharm. 2015; 12(11):4077-4084.

25. Sadia M, Sosnicka A, Arafat B, Isreb A, Ahmed W, Kelarakis A, Alhnan MA. Adaptation of pharmaceutical excipients to FDM 3D printing for the fabrication of patient-tailored immediate release tablets. Int J Pharm. 2016; 513(1-2):659-668.
26. Goyanes A, Robles Martinez P, Buanz A, Basit AW, Gaisford. Effect of geometry on drug release from 3D printed tablets. Int J Pharm. 2015; 494(2):657-663.
27. Chai X, Chai H, Wang X, Yang J, Li J, Zhao Y, Cai W, Tao T, Xiang X. Fused Deposition Modeling (FDM) 3D Printed Tablets for Intragastric Floating Delivery of Domperidone. Sci Rep. 2017; 7(1):2829.
28. Melocchi A, Parietti F, Maroni A, Foppoli A, Gazzaniga A, Zema L. Hot-melt extruded filaments based on pharmaceutical grade polymers for 3D printing by fused deposition modeling. Int J Pharm. 2016; 509(1-2):255-263.
29. Koland M, Sandeep VP, Charyulu NR. Fast Dissolving Sublingual Films of Ondansetron Hydrochloride: Effect of Additives on in vitro Drug Release and Mucosal Permeation. J Young Pharm. 2010; 2(3):216-222.
30. Rana P, Murthy RS. Formulation and evaluation of mucoadhesive buccal films impregnated with carvedilol nanosuspension: a potential approach for delivery of drugs having high first-pass metabolism. Drug Deliv. 2013; 20(5):224-235.
31. Mukherjee D, Bharath S. Design and characterization of double layered mucoadhesive system containing bisphosphonate derivative. ISRN Pharm. 2013:604690.
32. Abo Enin HA, El Nabarawy NA, Elmonem RA. Treatment of Radiation-Induced Oral Mucositis Using a Novel Accepted Taste of Prolonged Release Mucoadhesive Bi-medicated Double-Layer Buccal Films. AAPS Pharm Sci Tech. 2017; 18(2):563-575.
33. Prodduturi S, Manek RV, Kolling WM, Stodghill SP, Repka MA. Solid-state stability and characterization of hot-melt extruded poly(ethylene oxide) films. J Pharm Sci. 2005; 94(10):2232-2245.
34. Mantzavinos D, Hellenbrand R, Livingston AG, Metcalfe IS. Catalytic wet air oxidation of polyethylene glycol. Appl Catal B. 1996; 11:99-119.
35. Repka MA, Gutta K, Prodduturi S, Munjal M, Stodghill SP 2005. Characterization of cellulosic hot-melt extruded films containing lidocaine. European Journal of Pharmaceutics and Biopharmaceutics 59(1):189-196.
36. Repka MA, McGinity JW. Bioadhesive properties of hydroxypropylcellulose topical films produced by hot-melt extrusion. J Control Release. 2001; 70(3):341-351.
37. Selmin F, Franceschini I, Cupone IE, Minghetti P, Cilurzo F. Aminoacids as non-traditional plasticizers of maltodextrins fast-dissolving films. Carbohydr Polym, 2015; 115:613-616.
38. Lai F, Franceschini I, Corrias F, Sala MC, Cilurzo F, Sinico C, Pini E. Maltodextrin fast dissolving films for quercetin nanocrystal delivery. A feasibility study. Carbohydr Polym 2015; 121:217-223.
39. Chaudhary H, Gauri S, Rathee P, Kumar V. Development and optimization of fast dissolving oro-dispersible films of granisetron HCl using Box–Behnken statistical design. Bulletin of Faculty of Pharmacy, Cairo University. 2013; 51(2):193-201.
40. ElMeshad AN, El Hagrasy AS. Characterization and optimization of orodispersible mosapride film formulations. AAPS Pharm Sci Tech. 2011; 12(4):1384-1392.
41. BRITISH PHARMACOPOEIA COMMISSION, 2017. Appendix XII C. British Pharmacopoeia. London: TSO.

Table 1: The weight percentage compositions of various ingredients in 3D printed FDF formulations.

Formulation	PEO 100K	PEO 200k	PVA	Starch	Sodium Starch Glycolate	Croscarmellose	Ibuprofen	Paracetamol	SLS	Texture	Shape	Number of layers
A	58	-	-	20	-	-	20	-	2	Plain	Circle	1
B	-	58	-	20	-	-	20	-	2	Plain	Circle	1
C	-	40		18	-	-	40	-	2	Plain	Circle	1
D	-	45	-	-	10	2	-	42	1	Plain	Circle	1
E	-	-	80	-	-	-	-	20	-	Plain	Circle	1
F	-	-	63	-	-	7	-	30	-	Plain	Circle	3 (two taste masking layers*)
G	-	-	73	-	7	-	-	20	-	Mesh	Square	1
H	-	-	73	-	-	7	-	20	-	Mesh	Square	2 (one taste masking layer*)

*Taste Masking Layer=PEO 100K (80%), freeze-dried strawberry powder (20%).

PVA= Polyvinyl Alcohol

SLS= Sodium lauryl sulphate

PEO= Poly (Ethylene) Oxide

Table 2: Physical characteristics and disintegration time of 3D-FDFs (n=3)

Film	Thickness ± SD (µm)	Weight ± SD (mg)	*Nominal Drug Content Mean± SD (mg)	*Nominal Drug Content (%)	Disintegration Time ± SD (s)
A	242 ± 4	70.5 ± 0.7	13.9 ± 0.7	20	103 ± 9
B	246 ± 8	67.4 ± 0.8	14.5 ± 0.5	20	120 ± 5
C	235 ± 5	66.9 ± 0.7	24.8 ± 1.6	40	125 ± 11
D	245 ± 5	52.6 ± 1.3	27.1 ± 1.2	42	122 ± 6
E	374 ± 16	75.7 ± 2.2	15.1 ± 0.4	20	88 ± 21
$F	885 ± 31	344.6 ± 58.7	24.5 ± 0.3	7	150 ± 25
G	197 ± 21	42.6 ± 1.7	8.5 ± 0.3	20	42 ± 7
**H	298± 15	81.1 ± 4.8	8.5 ± 0.3	11	48 ± 5
Listerine® breath strips	45 ± 6	33.6 ± 0.3	-		14 ± 2

*The nominal content was calculated based on the weights of minimum 5 films for each formulation.

$These films had three layers, one drug containing layer and two taste masking layers (no drug). The drug containing layer weighed 81.6 ± 0.9 mg.

**These films had two layers, one drug containing layer and one taste masking layer (no drug). The drug containing layer weighed 42.6 ± 1.7 mg.

Figure 1

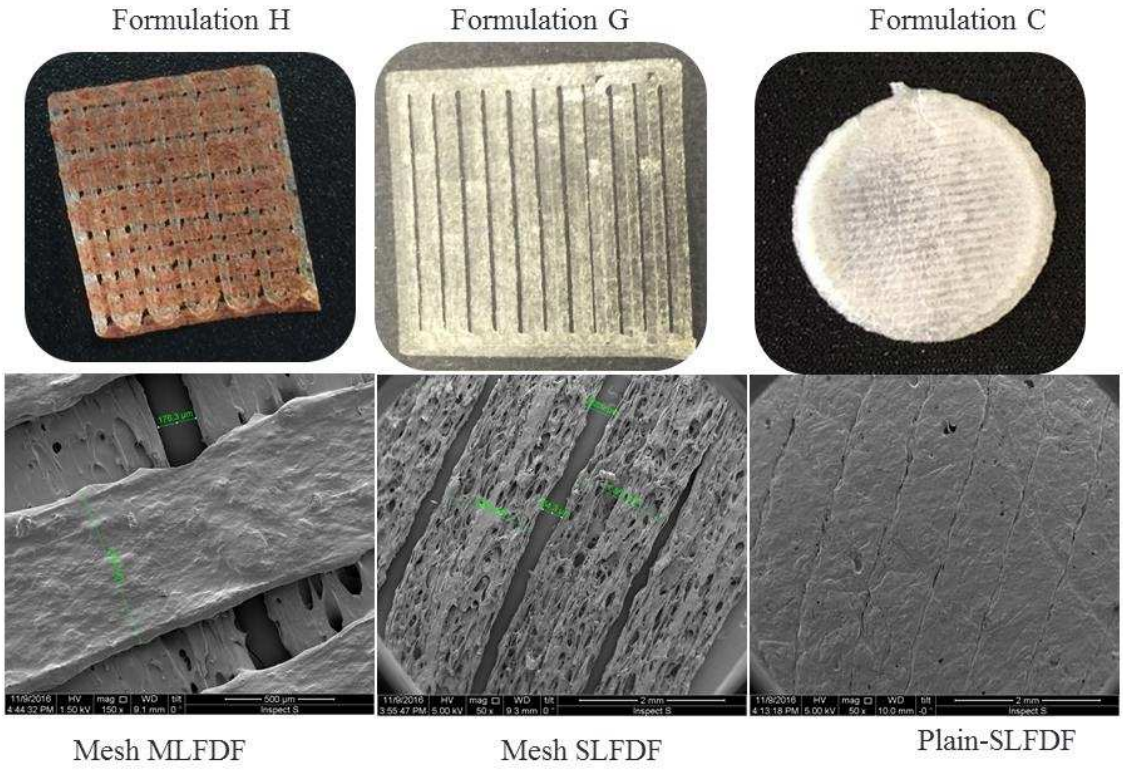

Figure 2A

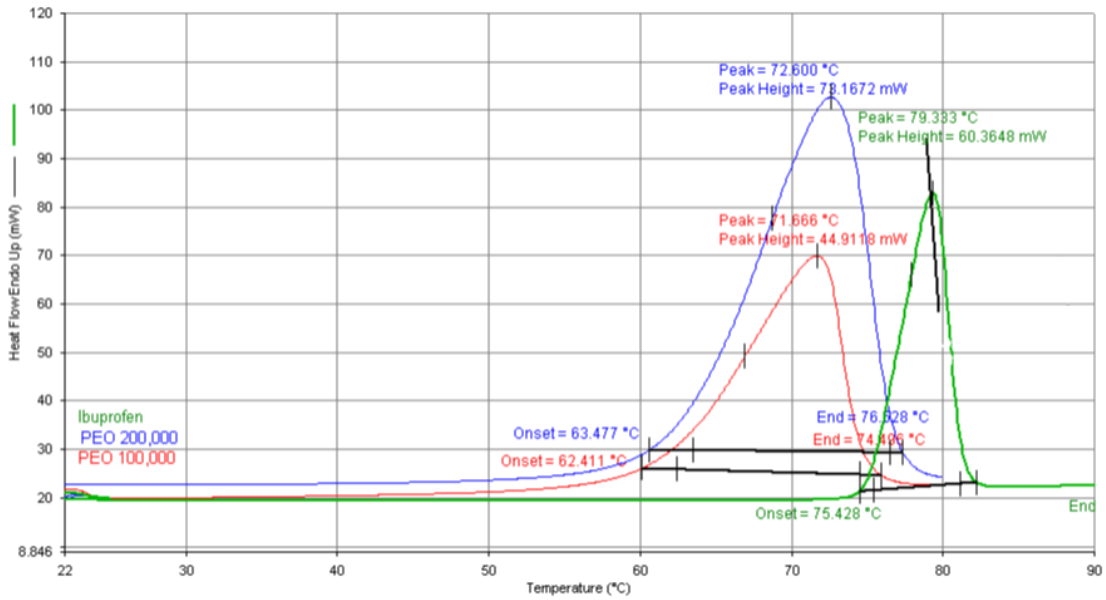

Figure 2B

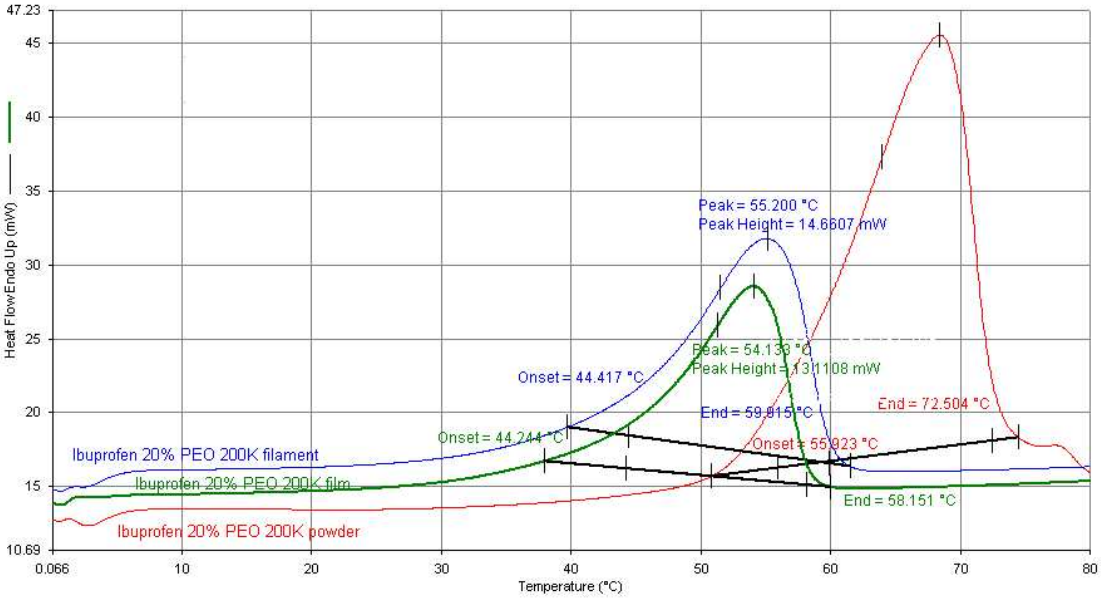

Figure 3A

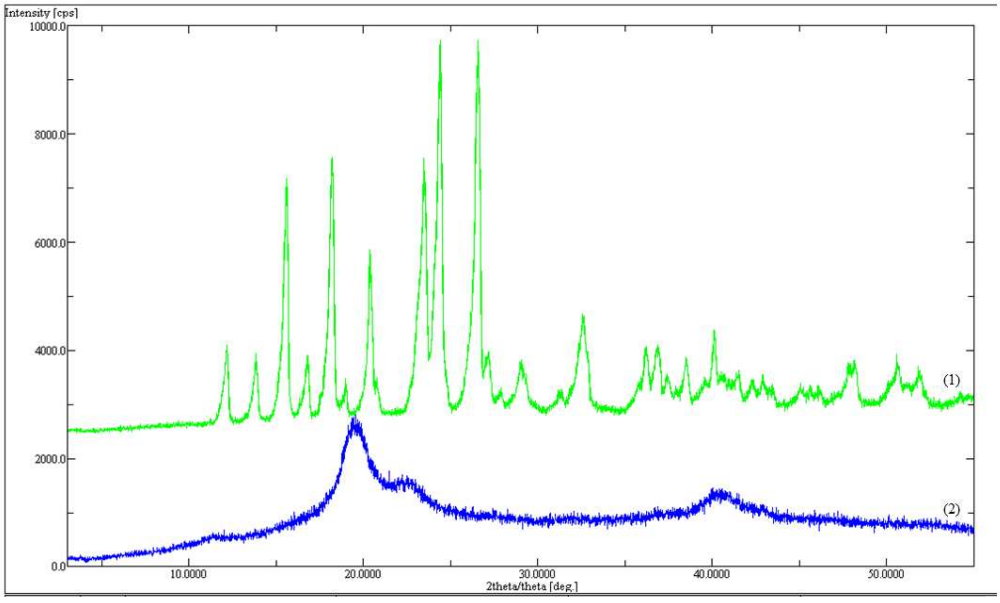

Figure 3B

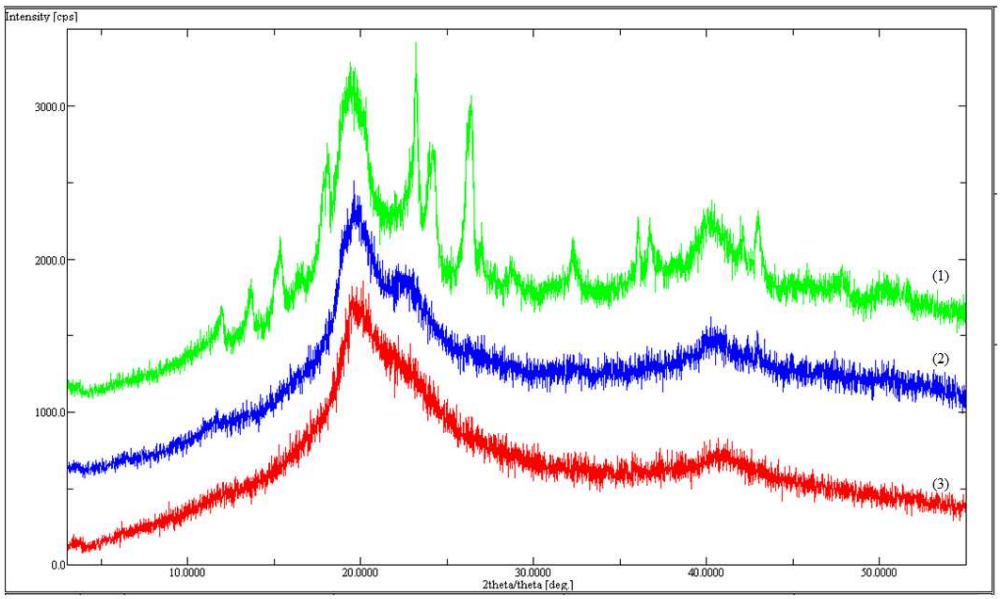

Figure 4

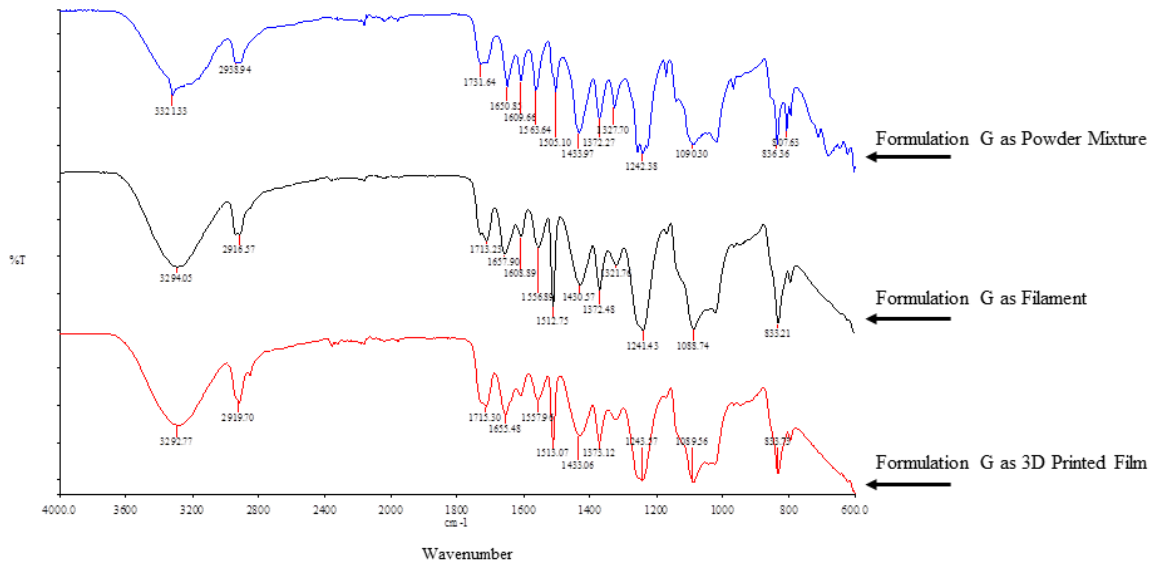

Figure 5

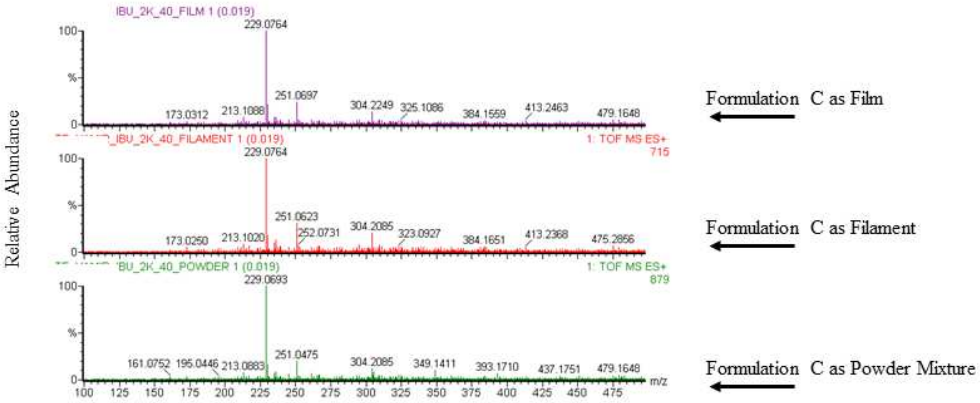

Figure 6

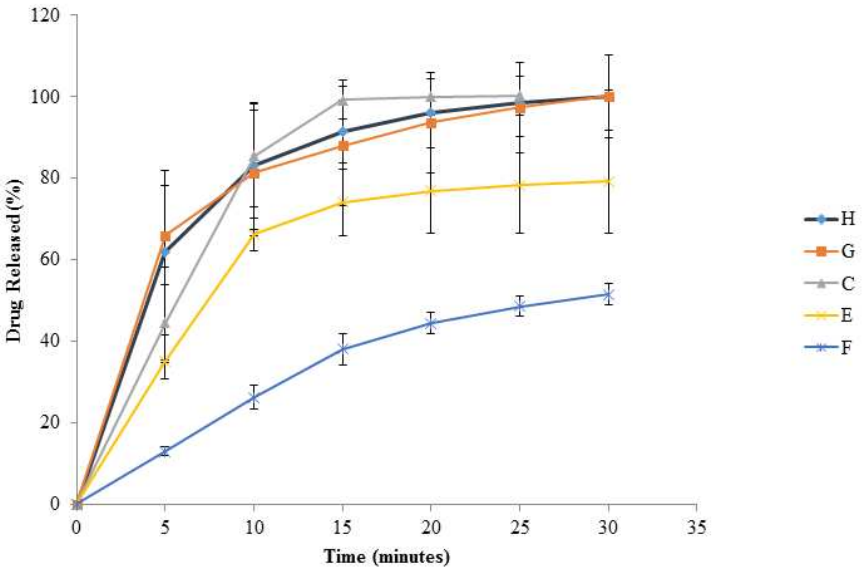

Figure 7

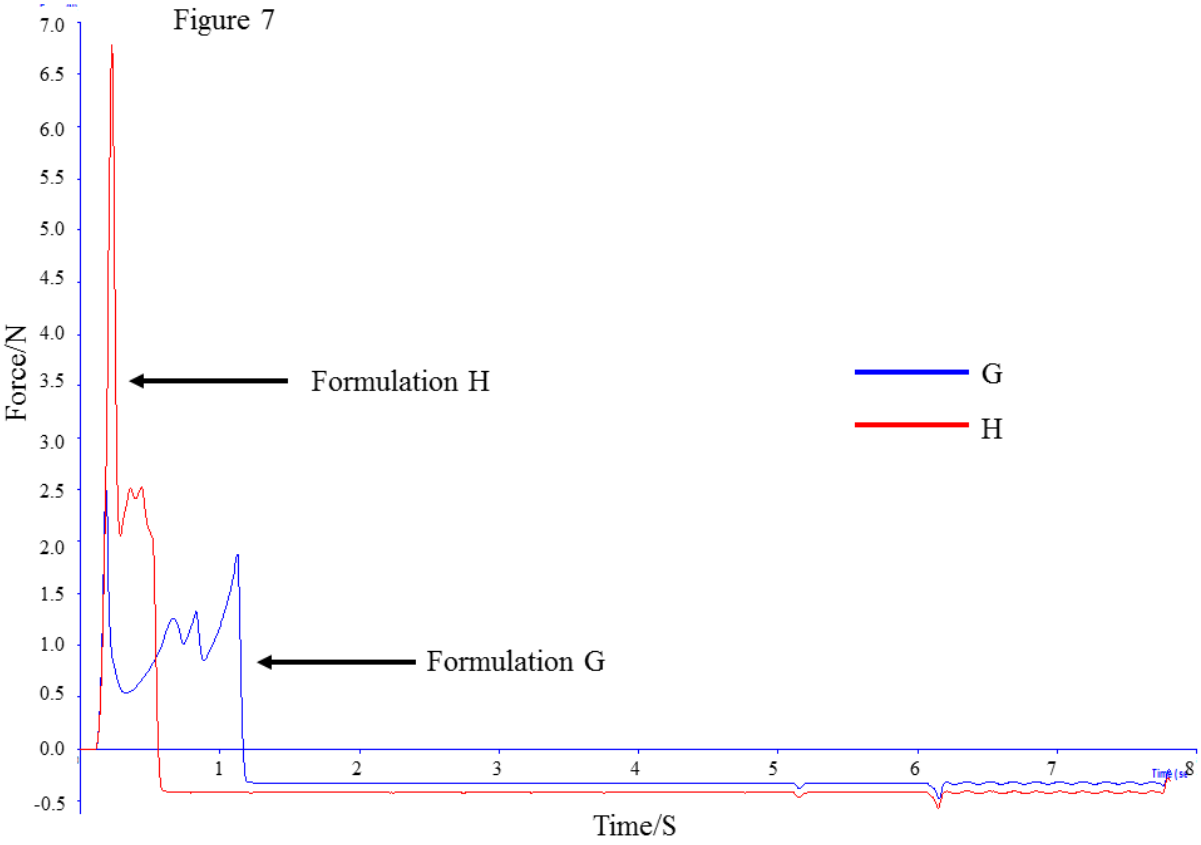
Force/N
7.0
6.5
6.0
5.5
5.0
4.5
4.0
3.5
3.0
2.5
2.0
1.5
1.0
0.5
0.0
-0.5
1
2
3
4
5
6
7
8
Time/S
Formulation H
Formulation G
G
H

Supplementary Information

The Application of 3D Printing in the Formulation of Multilayered Fast Dissolving Oral Films

Touraj Ehtezazi*, Marwan Algellay, Yamir Islam, Matt Roberts, Nicola M Dempster, Satyajit D Sarker,

School of Pharmacy and Biomolecular Sciences, Liverpool John Moores University, Byrom Street, Liverpool, L3 3AF, UK.

Supplementary information

DSC data

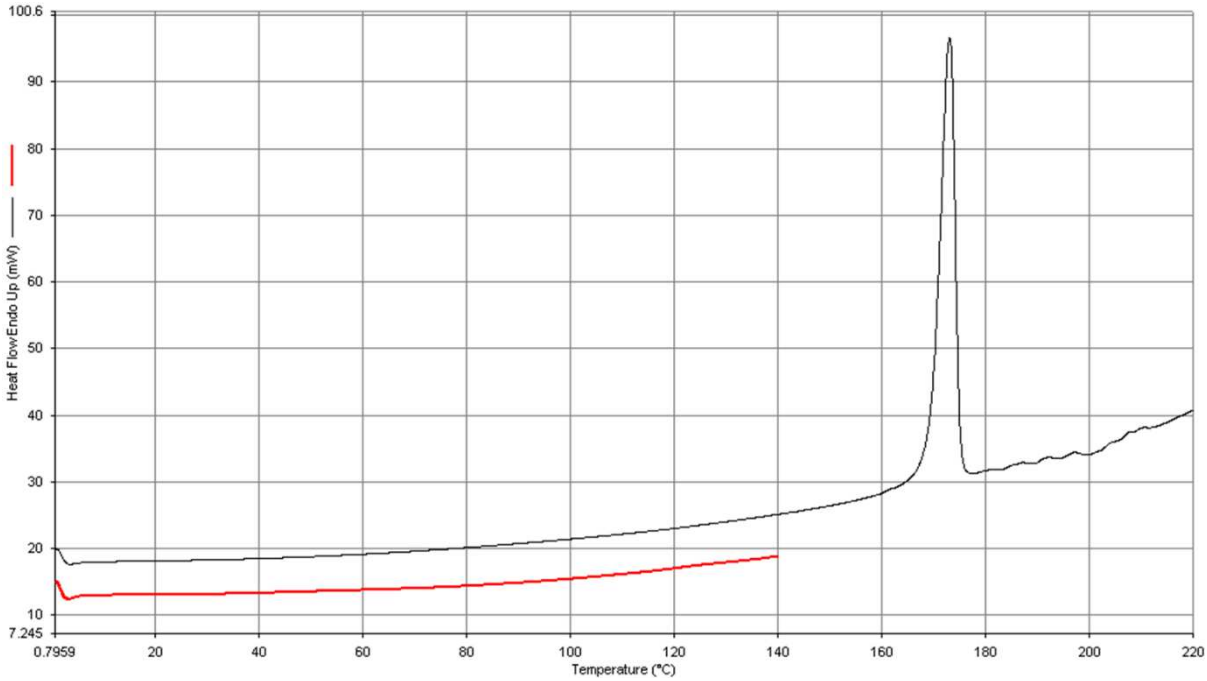

Figure S1. DSC thermogram of pure paracetamol powder (the black line is the reheat to simulate the heating process in the 3D printer).

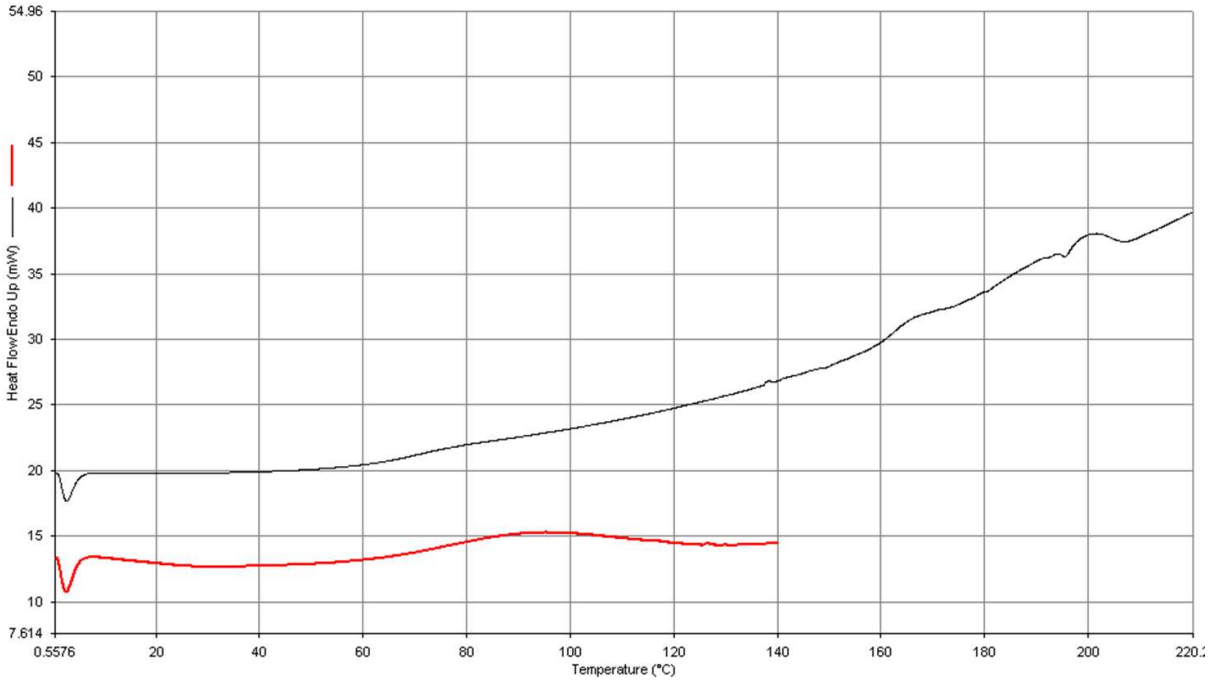

Figure S2. DSC thermogram of pure PVA powder (the black line is the reheat to simulate the heating process in the 3D printer).

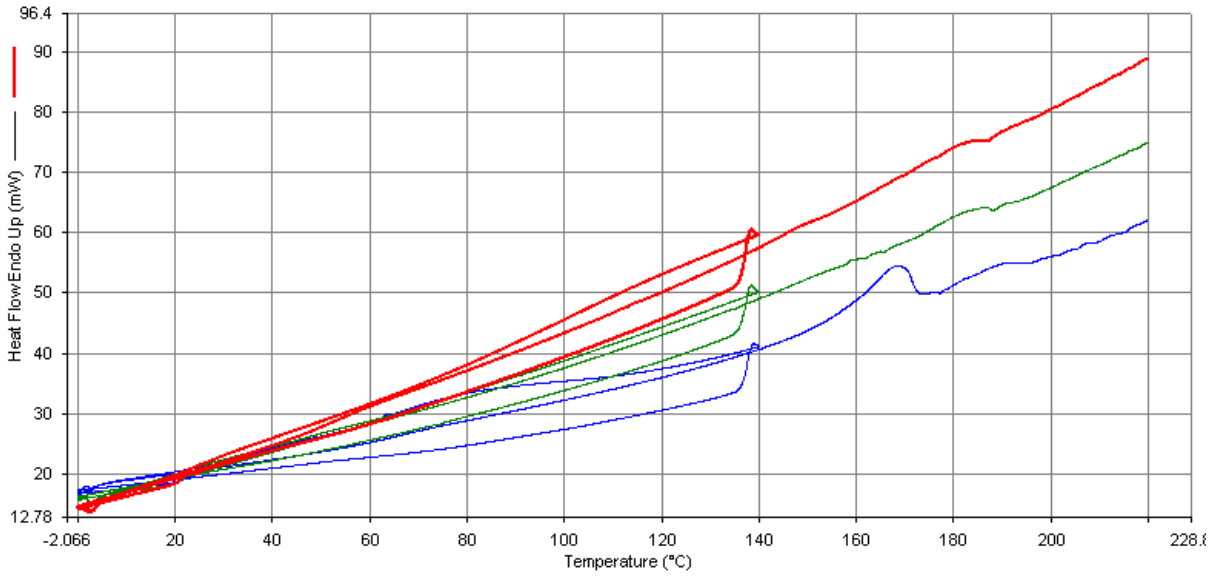

Figure S3. DSC thermograms of physical mixture of Formulation G (blue line), extruded filament of Formulation G (green line), and printed film of Formulation G (red line).

FTIR Data

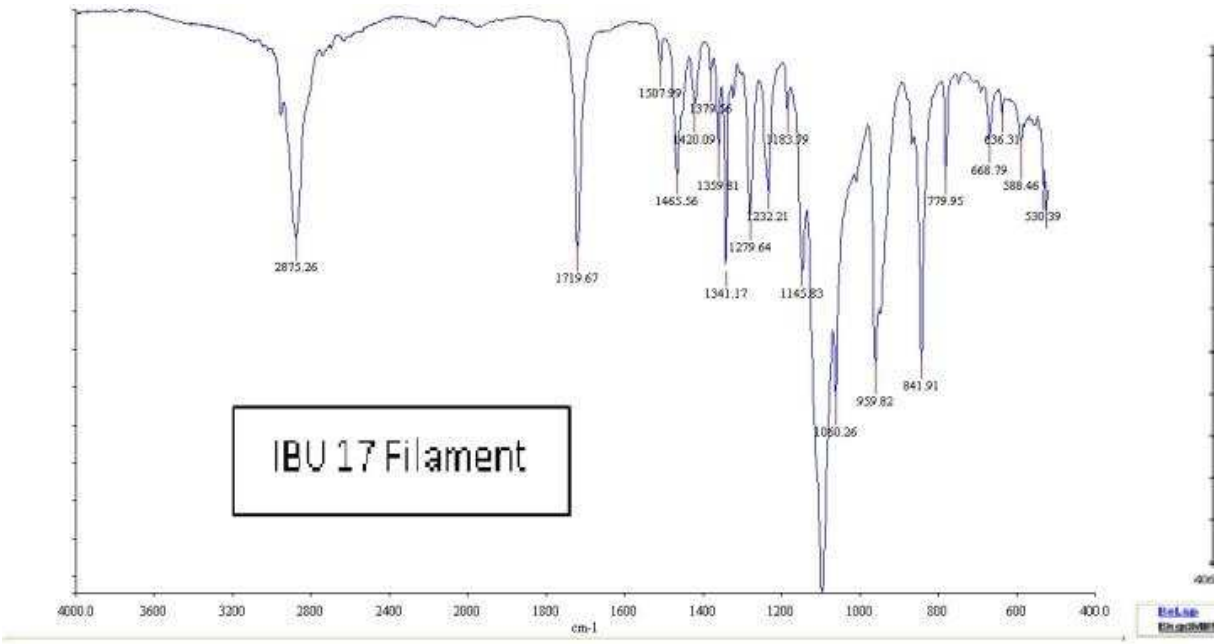

Figure S4. FTIR spectrum of formulation B as filament.

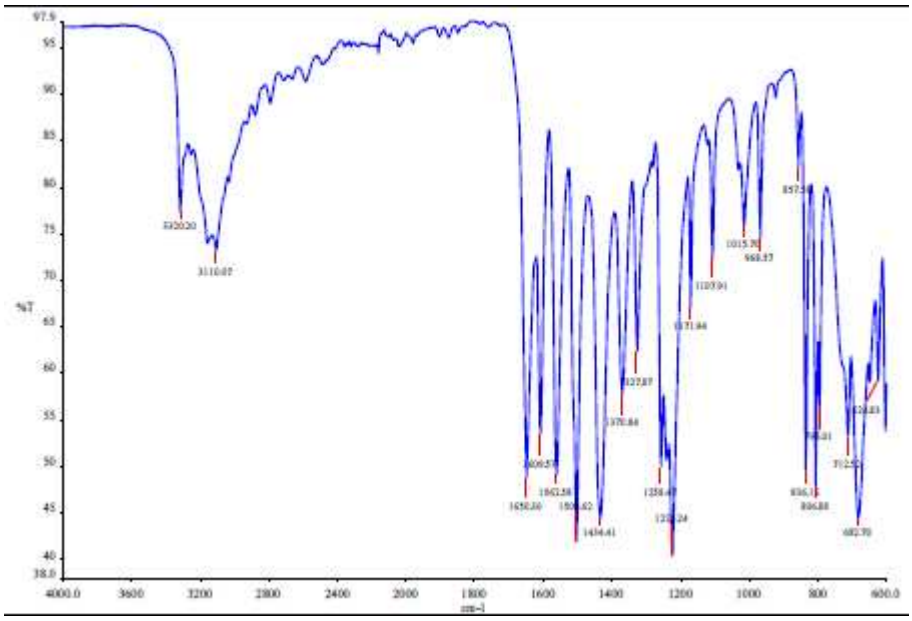

Figure S5. FTIR spectrum of pure paracetamol powder.

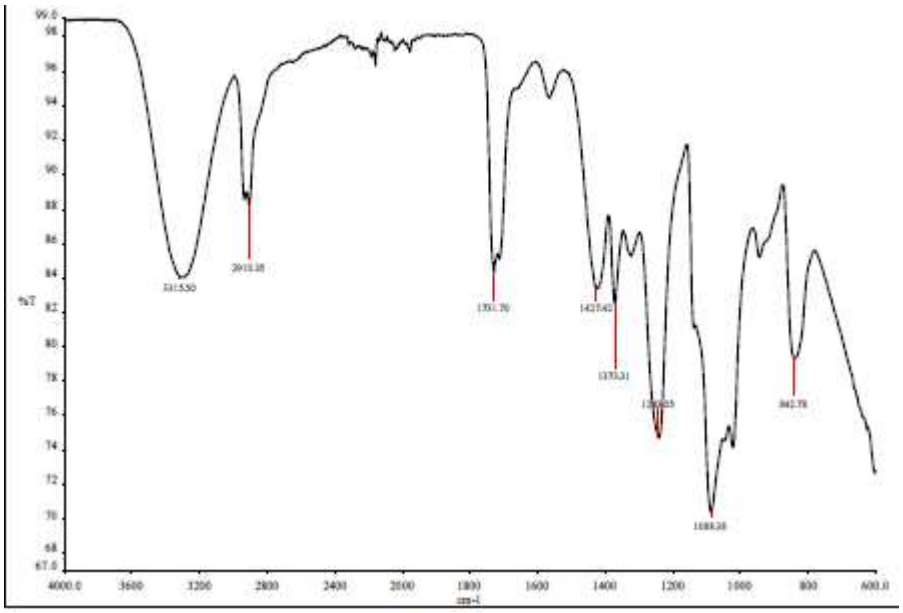

Figure S6. FTIR spectrum of pure PVA powder.

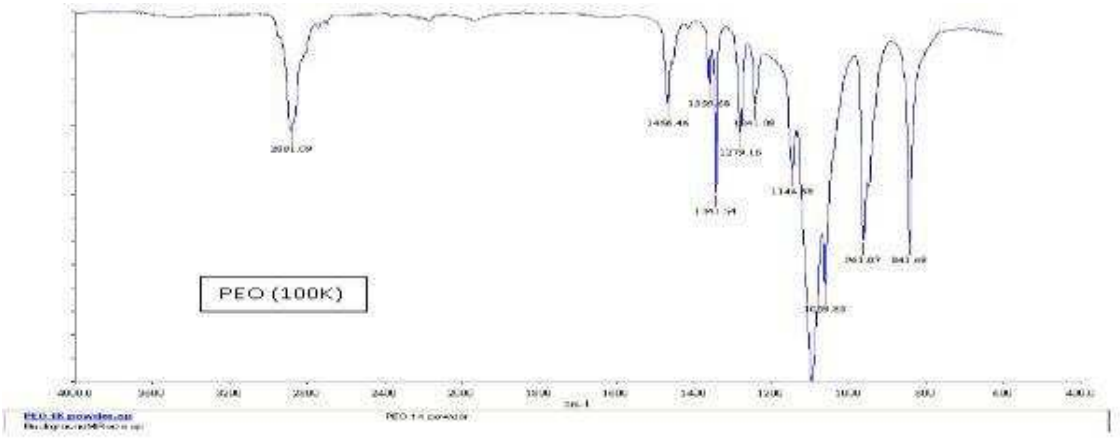

Figure S7. FTIR spectrum of pure PEO 100 kDa powder.

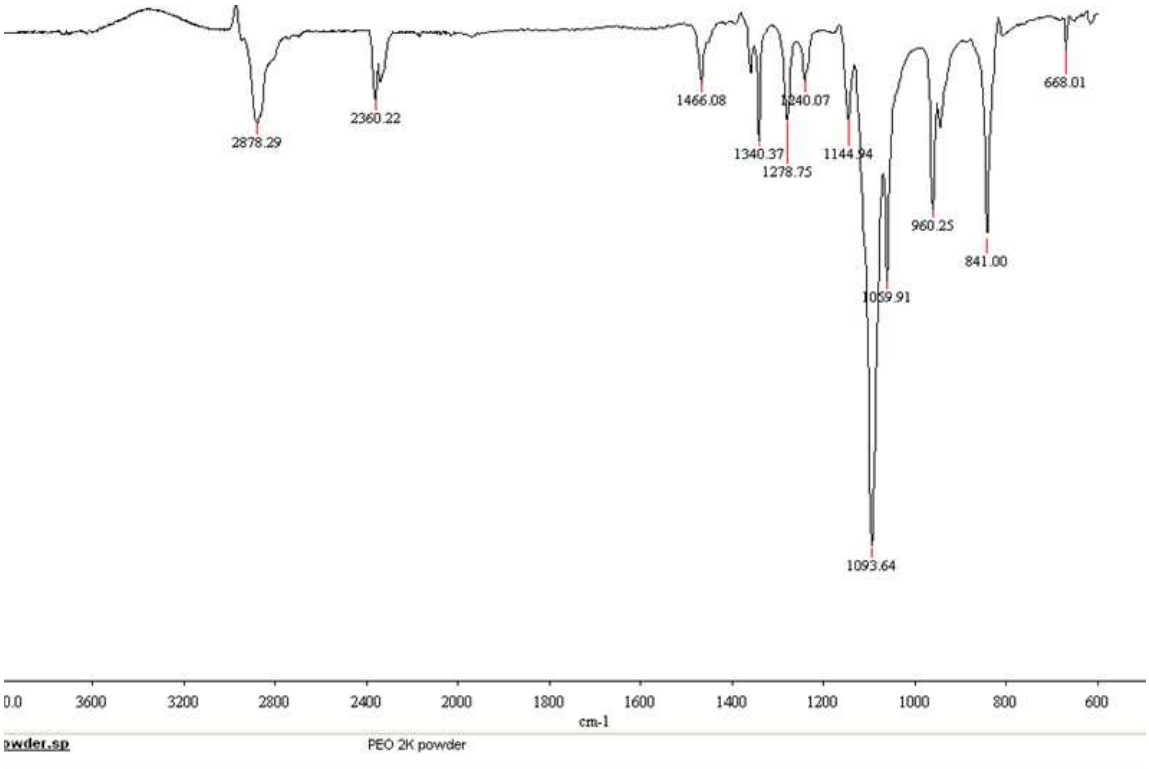

Figure S8. FTIR spectrum of pure PEO 200 kDa powder.

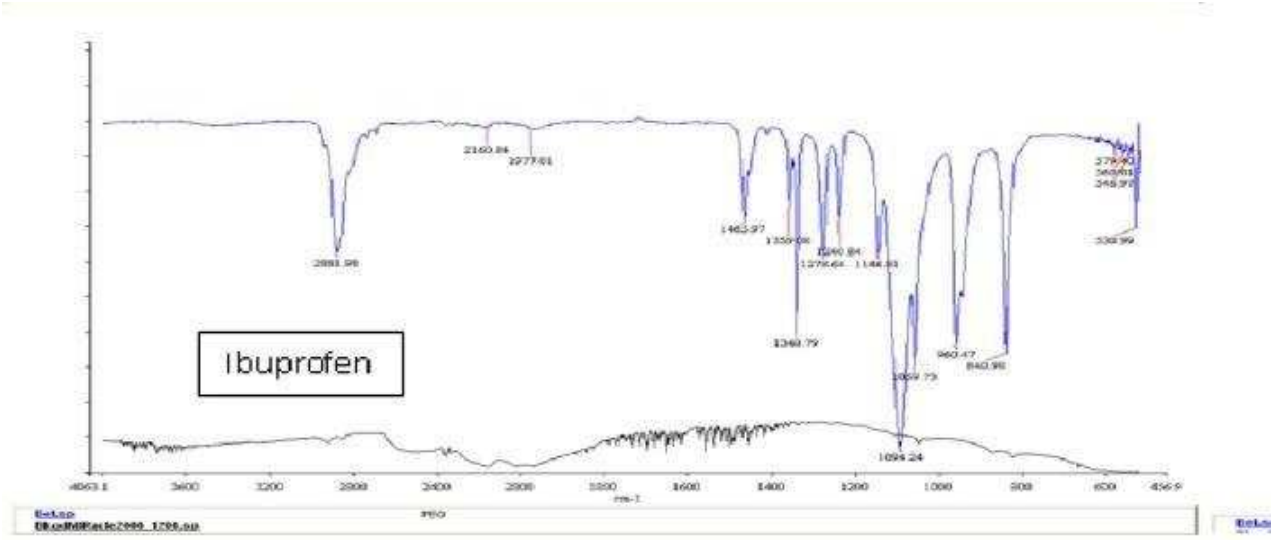

Figure S9. FTIR spectrum of pure ibuprofen powder.

LC-MS data

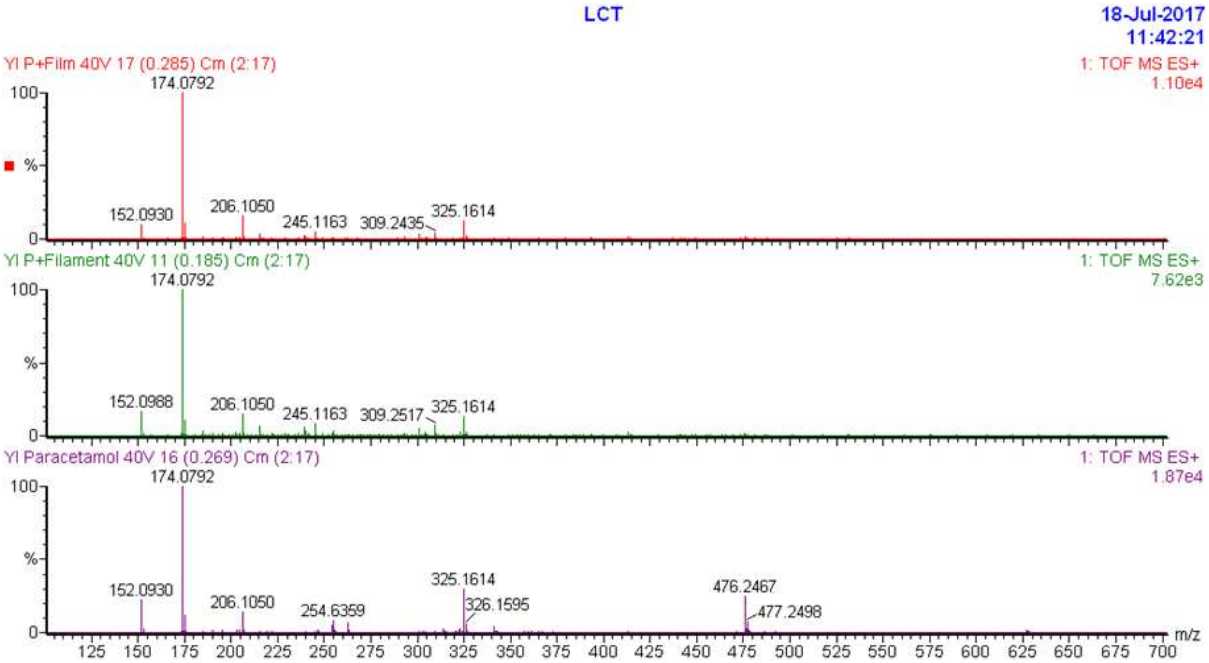

Figure S10. Mass spectra of paracetamol powder (pure active ingredient, bottom), and paracetamol in filament (middle) and film (top) for formulation E.

HPLC Data

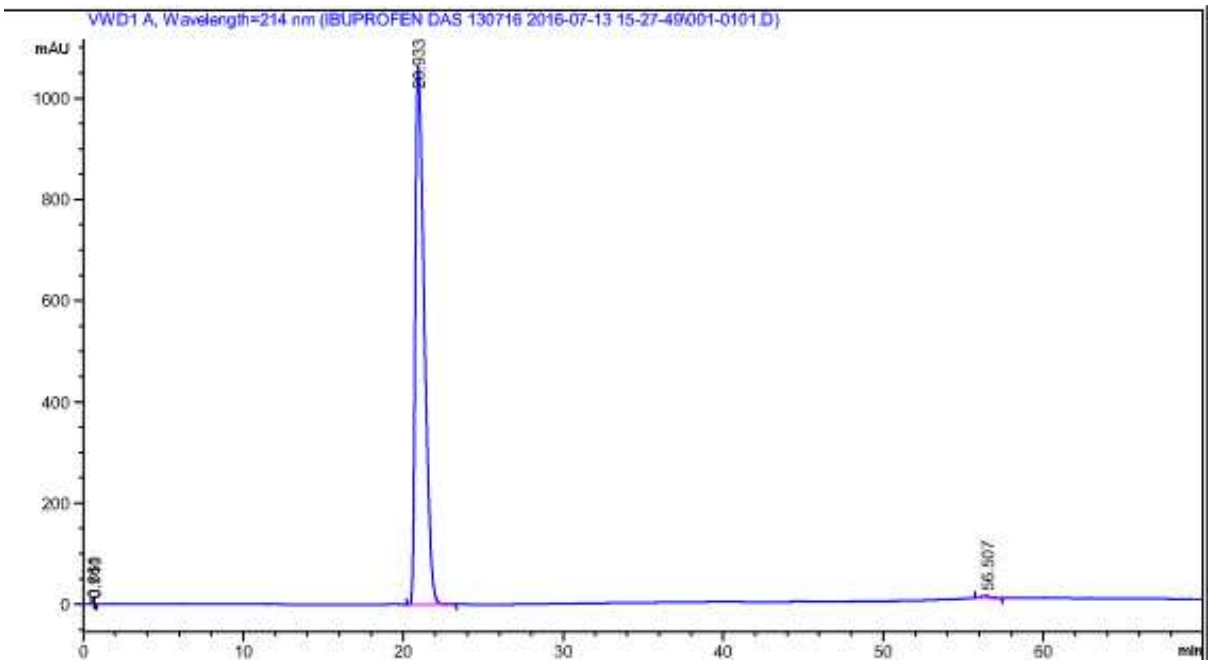

Figure S11. HPLC chromatogram of pure ibuprofen.

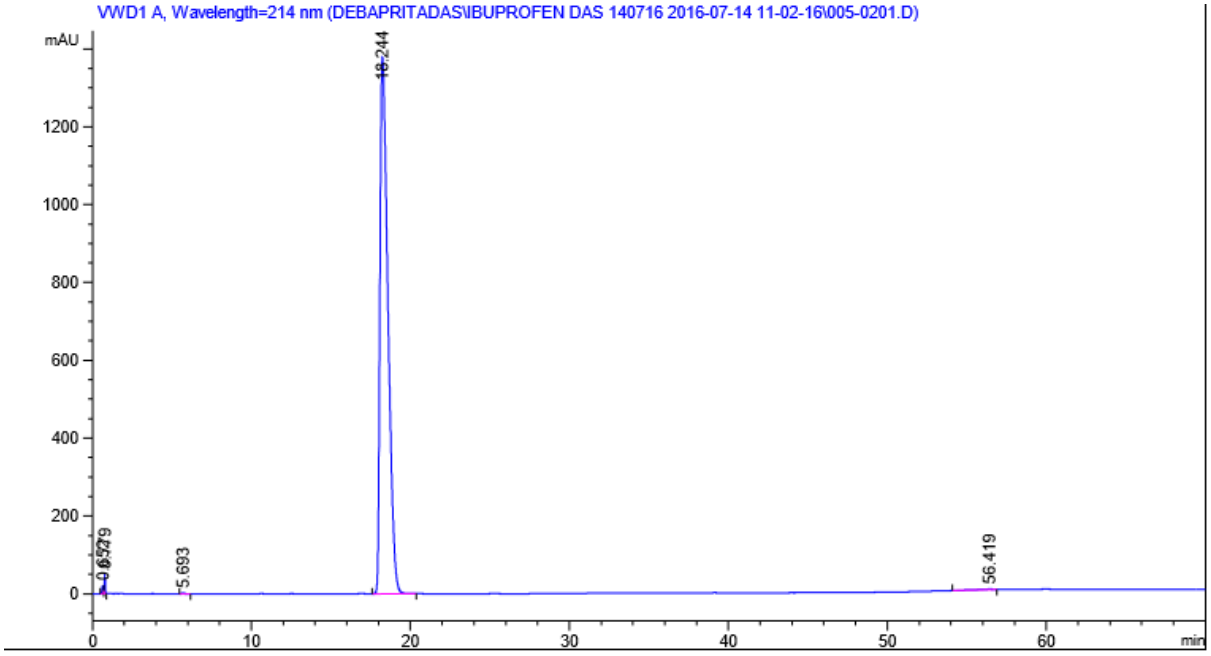

Figure S12. HPLC chromatogram of ibuprofen in filament with PEO 200 kDa (formulation B).

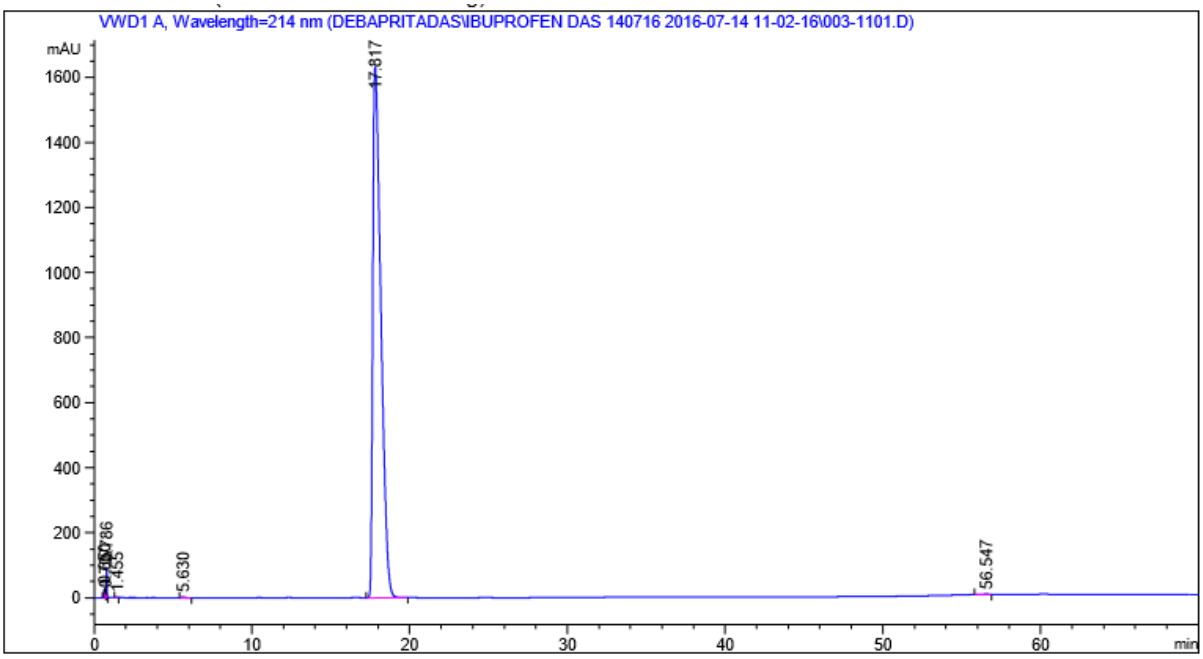

Figure S13. HPLC chromatogram of ibuprofen film printed at 165 °C (formulation B).

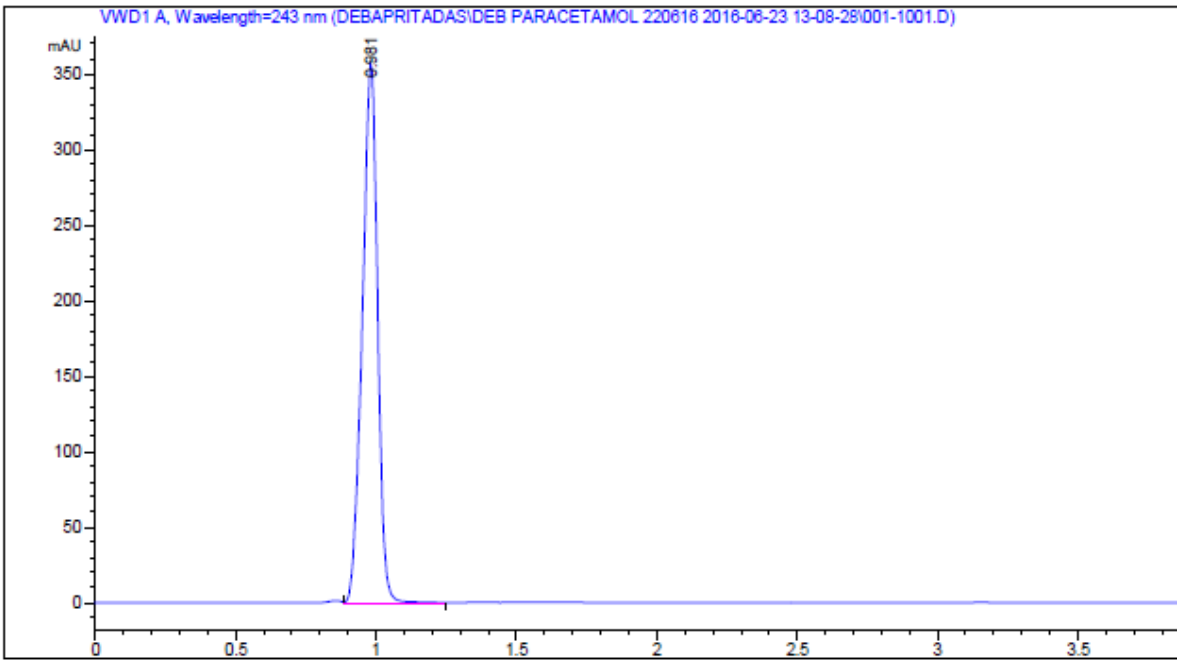

Figure S14. HPLC chromatogram of paracetamol powder.

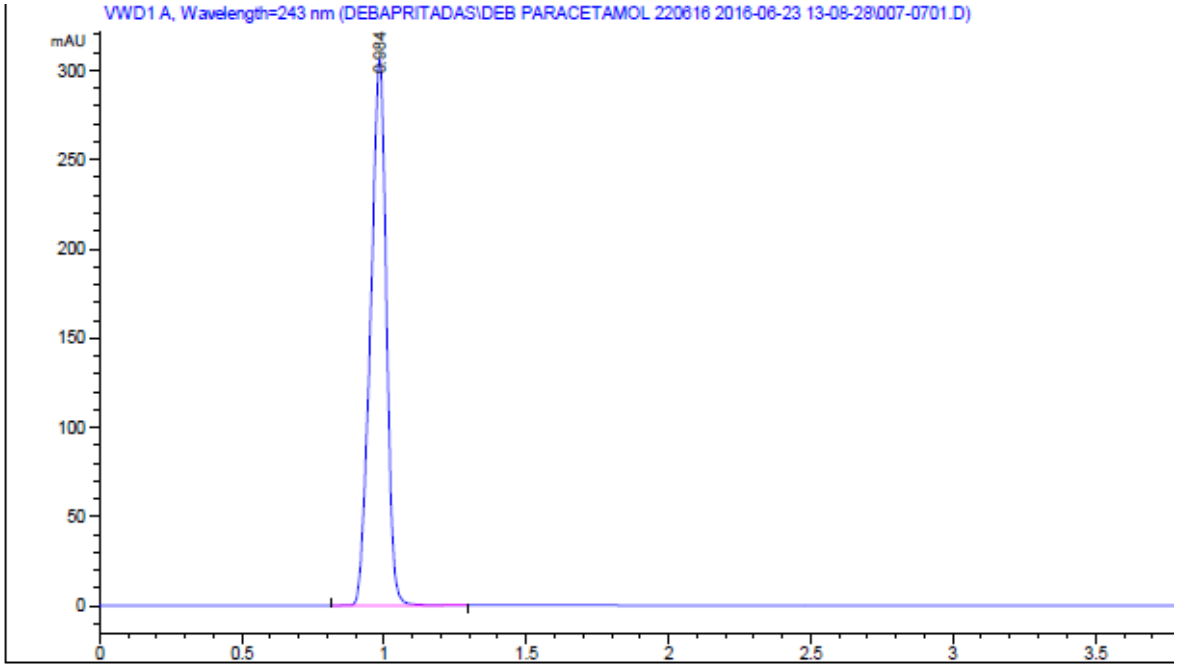

Figure S15. HPLC chromatogram of paracetamol printed film containing PEO 200 kDa (formulation D).

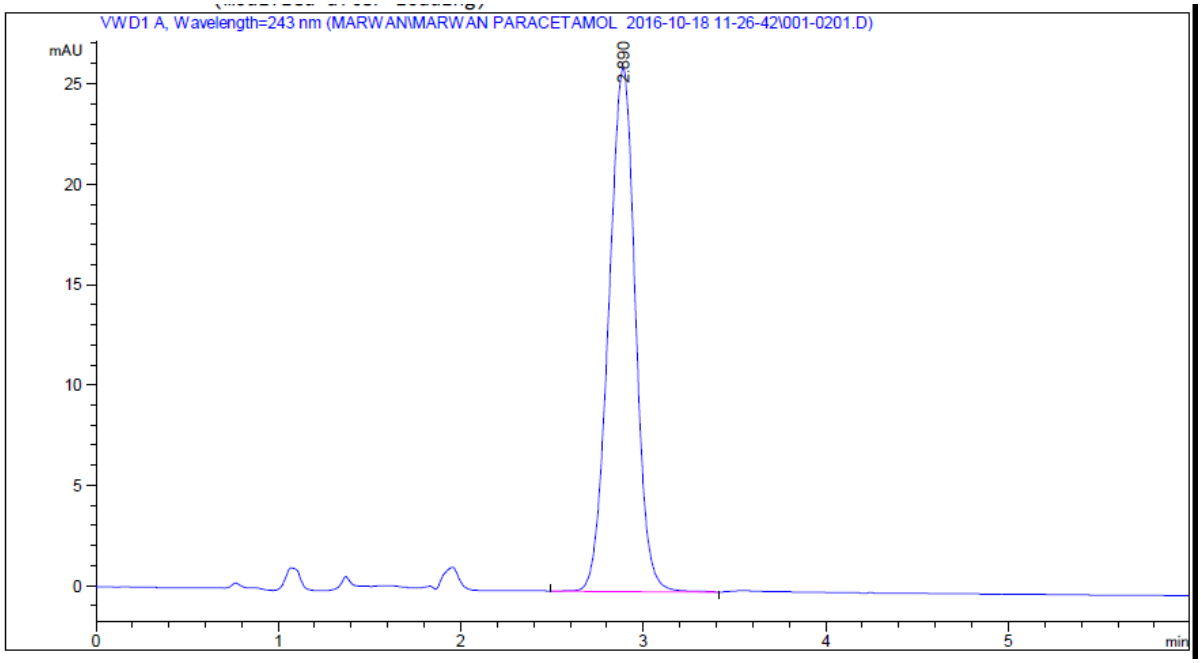

Figure S16. HPLC chromatogram of paracetamol standard powder, this was obtained separately while analysing formulation E films.

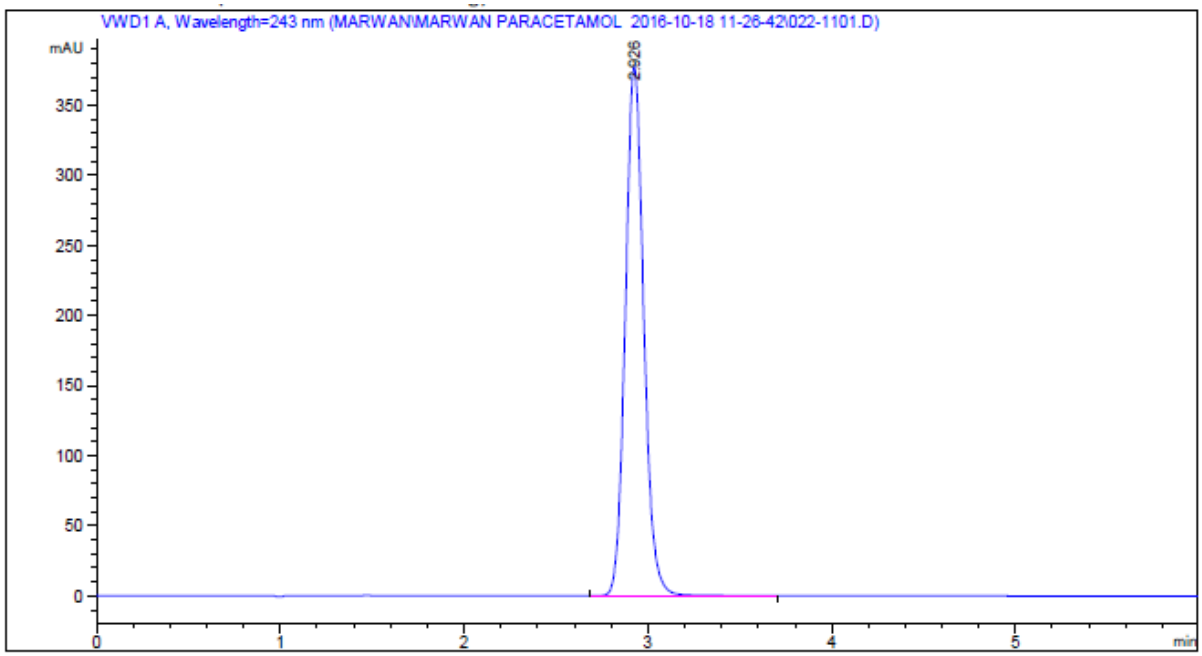

Figure S17. HPLC chromatogram of printed film containing paracetamol and PVA (formulation E).

Release Profiles

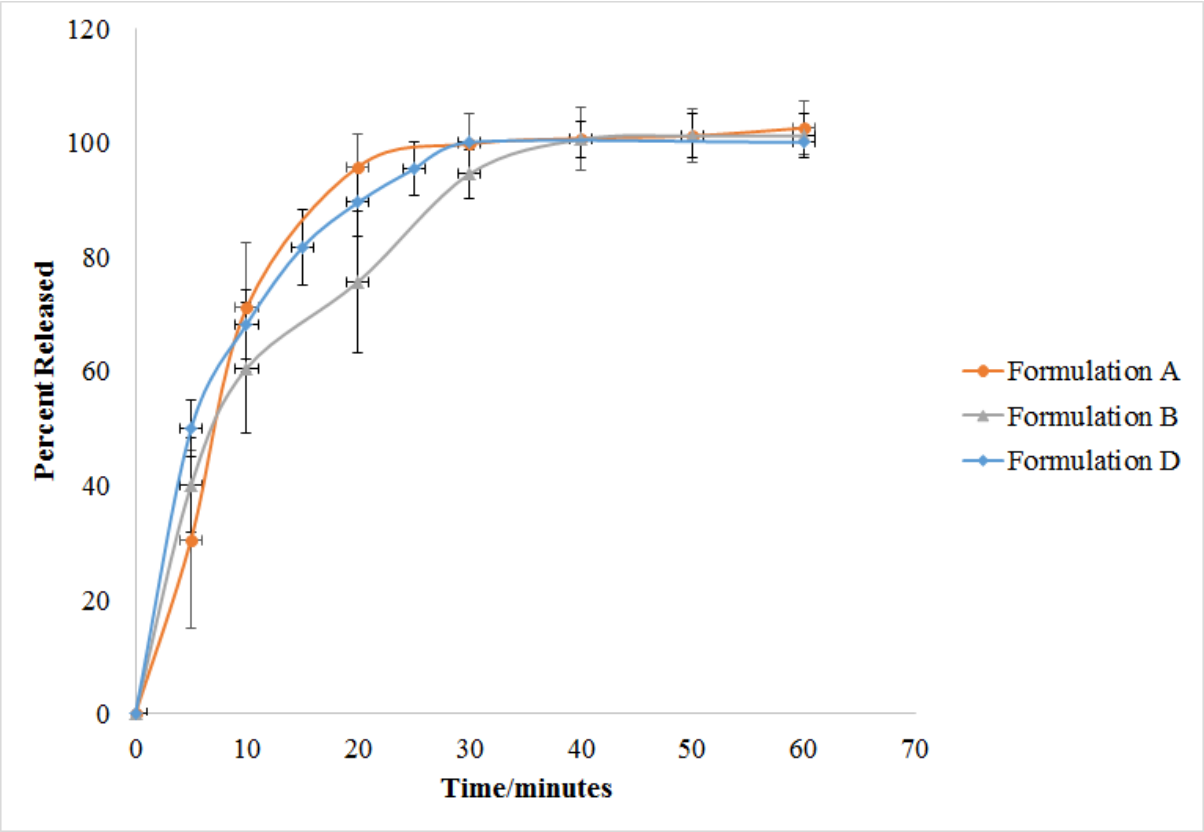

Figure S18. The release profiles of ibuprofen and paracetamol from films of formulations A, B and D. Bars indicate standard deviations (n=6).

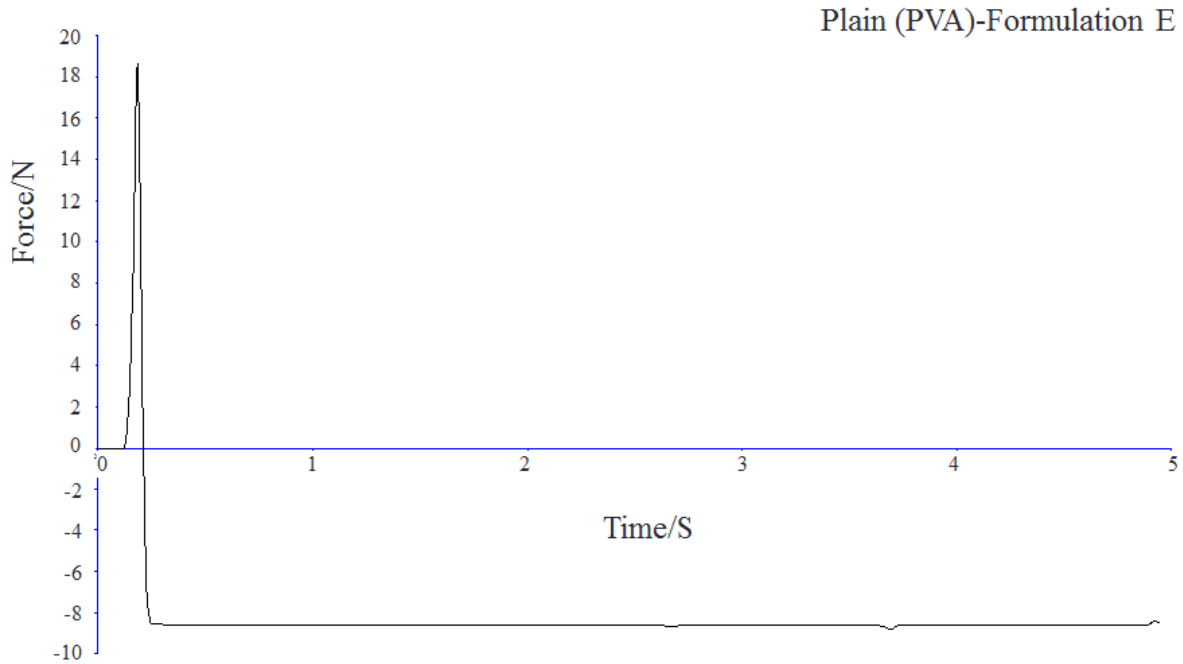

Figure S19. Texture profile analysis plot of formulation E.